ORIGINAL ARTICLE

Urban geochemistry of heavy metals in road dust from Cairo megacity, Egypt: enrichment, sources, contamination, and health risks

Mouataz Tarek Mostafa[1] · Habash El-Nady[2] · Ramadan Mohammed Gomaa[3] · Hany Fathy Abdelgawad[3] · Mahmoud A. Abdelhafiz[4] · Salman Abd Elraouf Salman[5] · Ibrahim Hussein Khalifa[6]

Abstract

Traffic emissions, overpopulation, and poor urban planning have degraded the environmental quality of the Greater Cairo megacity. As road dust is considered the main sink of pollutants in urban environments, thirty road dust samples from six major roads were collected. ICP-OES was used to analyze the samples in order to determine the contamination grade using the pollution indices, decipher metal sources and geochemical associations using multivariate analysis, and evaluate the ecological and human health risks. The average contents of heavy metals were arranged in decreasing order: Fe (1181.12), Zn (201.36), Pb (66.10), Ni (32.42), Cu (26.07), Cr (26.00), Co (14.78), As (2.76), and Hg (0.93) mg/kg. The spatial pattern showed that new urban communities exhibited lower contamination levels compared to unplanned old districts, especially for traffic elements (Pb, Zn, and Cu). The highest I_{geo} mean value was observed for Hg (3.34) followed by Zn (1.34), Pb (1.24), Ni (0.10), As (-0.19), Co (-0.24), Cu (-0.73), and Cr (-1.05). Additionally, CF values indicated very high contamination levels for Pb and Zn, whereas the highest PLI value was observed at Ramses Street. All EF values were higher than 1.5, indicating the anthropogenic enrichment of metals. RI values classified Cairo as a region with considerable ecological risk, observing that Hg was the main contributor. Correlation analysis and PCA showed that Pb and Zn originated from vehicle exhaust, Hg, Cu, and As from domestic and industrial activities, and Fe and Co from natural origin. Cr and Ni exhibited potential carcinogenic risks for children through ingestion; conversely, the non-carcinogenic risks were within safe levels. As a result, the use of clean energy is recommended to mitigate the accumulation of heavy metals in road dust and to improve the quality of life.

Keywords Environmental quality · Road dust · Heavy metals · Vehicle exhaust · Health risk assessment

✉ Mahmoud A. Abdelhafiz
   elkarim_mahmoud@azhar.edu.eg; abdelhafizma@gmail.com

   Mouataz Tarek Mostafa
   mouataz.t.mostafa@sci.aru.edu.eg

   Habash El-Nady
   dr.habash.elnady@gmail.com

   Ramadan Mohammed Gomaa
   ramgoma2@yahoo.com

   Hany Fathy Abdelgawad
   abdelgawadhany@gmail.com

   Salman Abd Elraouf Salman
   sal_man19@yahoo.com

   Ibrahim Hussein Khalifa
   ibrahim_khalifa@science.suez.edu.eg

1   Geology Department, Faculty of Science, Arish University, Giza 45511, Egypt

2   Geology Department, Faculty of Science, Arish University, Mansoura 35516, Egypt

3   Geology Department, Faculty of Science, Arish University, North Sinai 45511, Egypt

4   Geology Department, Faculty of Science, Al-Azhar University, Assiut Branch, Assiut 71524, Egypt

5   Geological Sciences Department, National Research Centre, Giza 12622, Egypt

6   Geology Department, Faculty of Science, Suez Canal University, Ismailia 41522, Egypt

Introduction

Urban geochemistry is a relatively new interdisciplinary science that provides a wealth of scientific knowledge about the geochemical characteristics of trace elements in the urban environment (e.g., concentrations, dispersion, fate, and sources) associated with intense human activities and the subsequent impacts on human health and environmental quality, in addition to the urban influence on biogeochemical cycles (Chambers et al. 2016). Moreover, the geochemistry of urbanized areas differs from the lithosphere due to the presence of heterogeneous mixtures of elements and synthetic materials at enriched levels in contact with natural earth materials. These mixtures can be degraded, making chemical and physical alterations of natural materials, with the aid of weathering and human activities (e.g., combustion) (Chambers et al. 2016; de Vos et al. 2002). Accordingly, various urban components produce higher fluxes of different elements, such as the association of concrete dissolution with increasing the levels of calcium and bicarbonates in urban streams (Bain et al. 2012), the leaching of Zn and Pb from building exterior materials (Davis et al. 2001), and the enrichment of Zn, Pb, and Cu in galvanized steel, which is used in pipes, wiring, and roofing materials as pure metals or in mixtures. Thus, all these processes distinguish the urban geochemical signature from the natural contributions of geogenic materials. Inappropriately, urban geochemistry is still underappreciated because of the limited awareness among administrations, especially in African megacities (Gardner et al. 2014).

Megacities are more vulnerable to environmental quality deterioration due to intensive human activities, which are usually accompanied by unplanned urbanization and high population growth rates (Fan et al. 2022; Zhang et al. 2018). Road dust (RD), the loose crustal material consisting of a mixture of mineral and organic particles, is considered a significant non-point source of heavy metal contamination in urbanized areas (Li et al. 2015). RD particles originate from the atmospheric deposition of solid materials, pavement abrasion, and wind-blown soil particles (Kasimov et al. 2020). These particles can be divided according to their source into two groups: (a) natural sources that can be attributed to natural geochemical processes such as road weathering, soil formation, and plant remains (Bernabé et al. 2005; Žibret 2019); (b) anthropogenic sources, which are mainly related to fossil fuel combustion, vehicle parts abrasion, and metallurgical activities (Guo et al. 2021; Said et al. 2019; Slezakova et al. 2007). Particularly, automobiles have been documented to be the main contributor of heavy metals (HMs) in RD as brake and tire wear produce nano-scale particles

containing Cu, Cd, Fe, Mo, Ni, and Zn (Adachi and Tainosho 2004; Elnazer et al. 2015; Žibret 2019). Significantly, RD is considered the main sink of pollutants in urban environments, accumulating on streets and sidewalks (Aguilera et al. 2021). Simultaneously, these accumulated pollutants can be a significant secondary source of pollution when released into urban environmental matrices (e.g., roadside soil, roadside plants, air, and surface water) by resuspension via wind and traffic or washing off by stormwater runoff (Zgłobicki et al. 2018). The resuspended RD, with its occurrence at low heights in the living zone of humans, plants, and animals, is a critical source of aerosol pollution in large cities (Almeida et al. 2006; Logiewa et al. 2020). Furthermore, due to its high chemical mobility, metals in RD can easily be dissolved in rainy conditions and enter urban drainage networks. Undesirably, HMs in RD can accumulate in human internal tissues via inhalation, unintentional ingestion, and dermal contact, disrupting the normal functions of human internal organs (Al-Shidi et al. 2021; Lu et al. 2014). For instance, exposure to Pb has been reported to cause adverse effects on the central nervous system (Van der Kuijp et al. 2013), whereas long-term exposure to Cd causes pulmonary adenocarcinomas and renal dysfunction (Zhang et al. 2013). Recent contamination evaluation and health risk assessment studies concerning HM levels in RD have been conducted in many cities, such as Tiruchirappalli in India (Suvetha et al. 2022), Mexico City in Mexico (Aguilera et al. 2021), Beijing in China (Men et al. 2021), Lublin in Poland (Zgłobicki et al. 2019), Lagos in Nigeria (Taiwo et al. 2020), Madrid in Spain (Miguel et al. 1997), and Delhi in India (Suryawanshi et al. 2016).

Greater Cairo (GC), the study area, is the most populous metropolitan area in the Middle East and was ranked as the sixth-largest city in the world in 2018 (Huzayyin & Salem 2013; United Nations 2016). Overpopulation with poor urban planning, a tremendous increase in motorized traffic volume with an inappropriate mass transportation network, and unplanned urban polluting industries were the main factors responsible for the degradation of environmental quality in GC. Masoud (2023) pointed out the increasing deterioration of air pollution in Egypt, especially in Greater Cairo, due to increased urbanization, vehicle emissions, and climate changes. The degree of contamination with HMs in household dust in Cairo ranges from considerably to very high contamination, which expose residents to the risk of cancer. The source of pollution with HMs may be traffic emissions and industrial activities (Gad et al. 2022). Both of road and house-dust in Alexandria and Kafr El-Sheikh HMs concentrations are spatially linked to traffic emissions, anthropogenic activities and population density. Children in Alexandria are facing cancer risk from the presence of Pb in house-dust (Jadoon et al. 2021). Correspondingly,

Cairo was classified as one of the most polluted cities in the world, with extremely poor air quality ranging between 10 and 100 times lower than world standards (Davies 2015; Gurjar et al. 2008; Kanakidou et al. 2011). Although many environmental studies have been conducted in GC, focusing on different environmental media such as air, soil, and the Nile River (Al-Afify et al. 2018; Ali et al. 1992; Hassan & Khoder 2017; Rovella et al. 2021), research on RD contaminants is limited in the study area, which makes this research of utmost importance to policymakers and the scientific community. Therefore, the overarching aim of this study was to provide a wider knowledge base regarding the relationship between vehicle and industrial emissions and urban planning on the one hand, and RD contamination with HMs on the other. Thus, the present study was conducted to (a) appraise HM contents in the RD samples and elucidate the possible urban sources, (b) determine the contamination grade and assess the ecological risks, and (c) investigate the potential health impacts of these metals on adults and children via different exposure pathways. Hence, this study gives a preliminary evaluation of RD contamination with

HMs in GC, which will be useful in determining the degree of environmental deterioration and accordingly developing preventive and mitigating measures.

Materials and methods

Study area and sampling

Greater Cairo (GC) (Fig. 1), which administratively includes three governorates: Cairo (the capital of Egypt), Giza, and Qalyubia, is the largest urban area in the Middle East and North Africa (Abbass et al. 2020), with a total population of over 20 million people and a population density of about 34,640 inhabitants per square kilometer (Mohammed et al. 2020). This population was centered around the banks of the Nile River, with a length of about 50 km and an area of about 200 km^2. Regarding the environmental issues, the daily fine particulate matter (PM2.5) levels were reported to be significantly above the WHO standards for air quality (Hassan & Khoder 2017), which is reflected in deaths
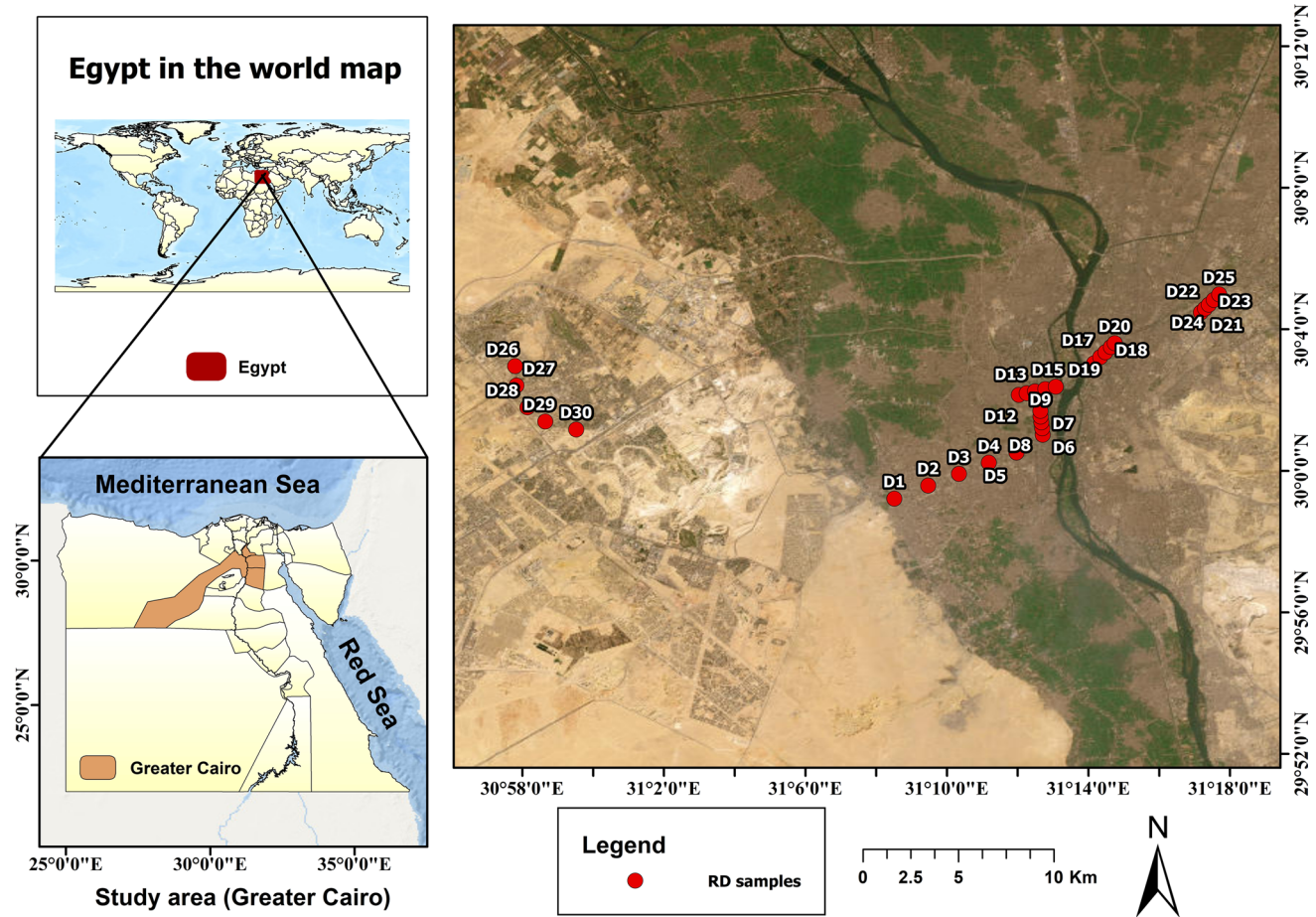

Fig. 1 Location of Greater Cairo, Egypt (the study area), and RD sampling points (D1-D30)

ranging between approximately 10,000 and 25,000 people annually due to air pollution-related diseases (Kanakidou et al. 2011). In general, air pollution sources in GC vary, including vehicle emissions, rubbish burning, and urban industrial activities. The lack of rainfall and wind erosion in the surrounding deserts encourage the accumulation of these pollutants (Wheida et al. 2018). Significantly, it has been proved that the stone materials used in carving and building Egyptian monuments were affected by environmental degradation resulting from atmospheric pollution (Rovella et al. 2021). Geologically, Cairo is covered by a thick sedimentary sequence from the Eocene up to the Quaternary, which is dominated mainly by the Quaternary alluvial deposits of the Nile River, the Tertiary marine carbonates of the ancient Mediterranean Sea, and the terrestrial quartzitic sandstone (Davies 2015). Notably, limestone is the essential building material in Egypt.

A total of 30 RD samples (D1-D30) were collected from six main roads in Greater Cairo, and each road was divided into five stations (Fig. 1). Each sample was a composite of five subsamples, mixed several times at each station to ensure that the sample was representative. Dust samples were gently swept using a polyethylene brush and plastic dustpan from the roads or pavement edges over an area of 1 m^2 and a weight of approximately 500 g for each sampling station. The dustpan and brush method, despite its simple nature, continues to be commonly employed in RD sampling (Idris et al. 2020; Kabir et al. 2021). Dust sweeping was conducted carefully to minimize the loss of fine particles, which can be easily re-suspended in the air (Ferreira-Baptista and De Miguel 2005). The brushes were cleaned with highly purified water and dried with a clean electric blow between each sample collection. Additionally, the sample collection points were chosen to be away from the construction activities and located within the main transport routes and popular activities to reflect the actual characteristics of the road (Table S1). For safety reasons, hand gloves and nose masks were worn, and sampling was conducted during the early morning hours to avoid rush-hour traffic. To study the impact of urban planning, samples (D26–D30) were collected from Sheikh Zayed City, one of the Egyptian new communities established as a planned urbanized area without traffic congestion, dense population, or uncontrolled industrial activities. Sample coordinates were taken using a portable global positioning system (GPS Garmin *eTrex* 30). Particularly, samples were collected during the summer, when the climate is dry and sunny, to avoid the role of rainfall in washing out RD. All samples were sealed, labeled, and bagged in clean polyethylene bags, and afterward they were allowed to dry at room temperature for 3 days to drive out any moisture. Eventually, these samples were sieved through a 63-μm sieve and then crushed to a fine powder using an agate mortar for further analysis. This particle grain size was chosen because it can be easily resuspended and remain airborne for considerable durations (Shilton et al. 2005), causing higher risks to human health than the coarser fractions (Najmeddin et al. 2018).

Geochemical analysis and quality assurance

Microwave digestion systems are a commonly used technique for sediment sample digestion (Bourliva et al. 2017). To clarify, 0.5 g of homogenized RD sample was weighed and transferred to PTFE vessels. Afterward, 9 ml of nitric acid (69%) and 1 ml of hydrogen peroxide were added to the sample, and then the vessel was closed completely and transferred to the microwave. A temperature-controlled program was used to conduct digestion in the microwave oven, including three stages: heating to 200 °C for 15 min, holding time for 15 min, and cooling to 85 °C for 15 min. After cooling to room temperature, the vessel's contents were transferred to a volumetric flask (25 mL) and diluted to the mark with ultrapure water for further analysis. The same digestion procedures were followed by Abou El-Anwar et al. (2022). Total concentration for selected HMs (Pb, As, Hg, Co, Cr, Ni, Cu, Zn, and Fe) was performed at the Department of Food Toxicology and Contaminants of the Egyptian National Research Centre using the Agilent 5100 Synchronous Vertical Dual View (SVDV) ICP-OES with Agilent Vapor Generation Accessory (VGA 77). Quality assurance (QA) and quality control (QC) included using reagents of high purity, reagent blanks, analytical triplicates, samples submission to the laboratory in random order, and the analysis of standard reference materials from the Merck Company (Germany) and the National Institute of Standards and Technology (NIST). The relative standard deviations (RSD%) of replicated samples ranged between 2 and 10%, whereas the recovery percentages varied from 89 to 112% for all tested metals. Moreover, the analytical precision was below 5%.

Descriptive and multivariate statistical analysis

Metal contents were expressed in terms of descriptive statistical analysis, including mean, median, maximum, minimum, standard deviation, and coefficient of variation. Pearson correlation coefficient was employed to elucidate the interrelationships between metal pairs, and principal component analysis was applied, using Varimax rotation and Kaiser normalization, to extract significant variables and distinguish similar metal sources. All statistics (descriptive and multivariate) and indices calculations were conducted using SPSS 23, Minitab 17, and Microsoft Excel 16 software packages, whereas the graphical representation of results was created using the Origin 2021 software package.

Pollution and ecological risk indices

Metal enrichment evaluation in different environmental matrices based only on comparing the total metal content with literature values is not a reliable method as it does not give holistic information about the contamination level; therefore, many recent studies have used pollution indices in studying the contamination of different environmental media (Abdelhafiz et al. 2021; Irshad et al. 2019, 2021; Jose and Srimuruganandam 2020; Malakootian et al. 2021). To deduce the pollution in road dust the following indices were applied.

The geo-accumulation index (I_{geo}) is calculated using the following equation (Muller 1969):

$$\left(I_{geo}\right)_n = \log_2\left(\frac{C_n}{1.5 \times B_n}\right) \tag{1}$$

In Eq. (1), C_n is the measured content of the target HM in RD samples (mg kg^{-1}), B_n is the content of the target HM in the background, and the constant (1.5) is a background matrix correction factor, which was employed to eliminate and correct the possible dissimilarities in the background values due to natural fluctuations of data or minor anthropogenic influences (Ekoa Bessa et al. 2022). The Upper Continental Crust, reported by Wedepohl (1995), were used as background values in this study (Table 1). Muller (1969) proposed seven classes of I_{geo}, as shown in Table S2.

Contamination factor (CF) is another individual index that is useful in terms of assessing sediment contamination and it is calculated as the ratio of the HM content in the RD sample (C_{sample}) to the corresponding reference level of this metal ($C_{background}$) (Eq. 2) (Hakanson 1980). An interpretation of CF values is presented in Table S3.

$$CF = \frac{C_{sample}}{C_{background}} \tag{2}$$

The pollution load index (PLI), introduced by Tomlinson et al. (1980), is useful in investigating the overall pollution risk by combining the impacts of all studied metals (Varol 2011). It depends on contamination factor values (CF) as shown in Eq. 3. Tomlinson et al. (1980) classified PLI into three grades to describe the level of deterioration in sediment quality (Table S4).

$$PLI = \left(CF_1 \times CF_2 \times CF_3 \times \cdots \times CF_n\right)^{\frac{1}{n}} \tag{3}$$

The enrichment factor (EF) is an efficient tool for evaluating anthropogenic contributions by allowing the distinction between natural and anthropogenic sources of heavy metals in studied samples (Wu et al. 2015). It is calculated using the following formula (Buat-Menard & Chesselet 1979; Sutherland 2000):

$$EF = \frac{\left(\frac{C_x}{C_{ref}}\right)\text{sample}}{\left(\frac{B_x}{B_{ref}}\right)\text{Background}} \tag{4}$$

where C_x is the measured concentration of the metal x in the sample, C_{ref} is the measured concentration of the chosen reference metal in the sample, B_x is the reference content of the HM in the background, and B_{ref} is the concentration of the selected reference metal in the background. In this study, Fe was used as a normalizing element. Generally, EF values less than 1.5 demonstrate that HMs are entirely derived from natural processes (e.g., weathering); conversely, if the value of EF exceeds 1.5, it means that the content of that HM was enriched due to anthropogenic sources (e.g., traffic emissions) (Sutherland 2000). A detailed interpretation of EF values is presented in Table S5.

The individual ecological risk factor (Er) was developed to integrate the ecological sensitivity and toxicity degree of HMs with their concentrations (Guo et al. 2012; Maanan et al. 2015; Kouchou et al. 2020). After that, the overall ecological risk (RI) caused by the combined impact of metals should be estimated by summing the potential individual risks (Er) (Kowalska et al. 2016; Luo et al. 2007). Hence, Er and RI indices can be quantitatively determined using the following formulas:

$$Er = T_r^i \times CF^i \tag{5}$$

$$RI = \sum_{i=1}^{n} Er \tag{6}$$

where Er is the individual ecological risk factor, T_r^i is the biological toxic factor for a specific toxic element (i) (Table S6), CF^i is the contamination factor of a specific metal (i), RI is the overall ecological risk index, and n is the number of measured metals. In this regard, the Er and RI categories, proposed by Hakanson (1980) are shown in detail in Table S7.

Health risk assessment model

The health risk assessment model is a commonly used procedure for evaluating human health risks (carcinogenic and noncarcinogenic) as a consequence of exposure to certain contaminants of known amounts (e.g., heavy metals and PAHs) through different exposure pathways (inhalation, ingestion, and dermal contact). It was developed by the US Environmental Protection Agency (USEPA 1989, 2004). Notably, the population was categorized into two categories: adults and children, due to their behavioral and physiological dissimilarities (USEPA 2002a). Humans are exposed to RD particles through ingestion (e.g., intended as in geophagy

Table 1 Basic statistical description of heavy metal concentrations in Greater Cairo dust samples (mg/kg)

Sites	Codes	Pb	As	Hg	Co	Cr	Ni	Cu	Zn	Fe
Haram	D1	51.9	3.18	1.001	12.94	25.95	25.29	71.46	197.59	1189.93
	D2	42.94	4.81	ND	14.15	22.81	13.05	63.16	181.07	1139.14
	D3	43.86	2.19	ND	13.91	19.86	20.97	55.18	161.79	1187.64
	D4	37.67	2.14	ND	13.61	24.71	25.86	4.17	179.97	1169.61
	D5	39.47	3.08	0.6	13.92	25.46	24.68	4.18	181.42	1190.81
	Mean	43.17	3.08	0.80	13.71	23.76	21.97	39.63	180.37	1175.43
Cairo University	D6	69.01	4.01	ND	14.66	26.09	9.48	80.60	232.64	1203.66
	D7	82.24	3.09	1.30	15.94	27.85	12.10	74.86	247.81	1235.42
	D8	95.09	2.15	0.29	17.58	36.35	32.98	78.61	240.88	1209.81
	D9	70.57	3.16	0.31	15.79	35.67	32.16	4.21	241.09	1208.37
	D10	80.11	3.36	0.67	15.38	32.18	31.54	4.22	227.40	1175.21
	Mean	79.40	3.15	0.64	15.87	31.63	23.65	48.50	237.96	1206.49
Tahrir	D11	69.87	3.04	1.18	13.72	27.44	26.98	49.43	210.45	1159.24
	D12	79.22	2.09	ND	15.90	28.14	33.83	46.88	253.01	1198.96
	D13	69.73	4.06	0.94	14.16	29.92	43.17	4.53	234.68	1142.72
	D14	69.10	2.4	ND	14.97	31.10	42.00	4.71	239.01	1195.22
	D15	66.21	3.25	1.28	14.79	31.41	41.25	4.70	227.11	1176.55
	Mean	70.83	2.97	1.13	14.71	29.60	37.45	22.05	232.85	1174.54
Ramses	D16	132.19	3.99	1.26	13.62	24.12	28.57	69.44	219.69	1095.85
	D17	112.47	3.93	1.10	13.72	30.43	34.99	41.52	274.19	1102.46
	D18	67.78	2.22	0.77	15.43	28.17	34.81	26.01	187.70	1113.42
	D19	131.78	3.18	1.35	14.46	36.69	47.46	4.93	221.52	1148.9
	D20	116.34	1.47	0.98	14.75	27.87	44.76	5.32	211.85	1166.77
	Mean	112.11	2.96	1.09	14.40	29.46	38.12	29.44	222.99	1125.48
El-Khalifa El-Maamoun	D21	64.94	2.94	0.92	12.88	22.47	22.4	28.64	206.22	1045.66
	D22	56.23	2.17	0.99	12.83	19.32	26.01	17.18	192.48	1096.38
	D23	60.77	2.82	0.66	12.22	26.31	51.18	4.62	191.24	1074.28
	D24	45.47	2.01	ND	12.45	23.15	47.75	5.11	189.12	1084.89
	D25	61.49	2.40	1.10	12.98	21.67	42.57	5.46	204.52	1128.01
	Mean	57.78	2.47	0.92	12.67	22.58	37.98	12.20	196.72	1085.84
Sheikh Zayed City	D26	44.17	2.09	0.60	18.87	16.93	29.69	4.40	141.56	1393.3
	D27	28.68	3.01	0.68	16.53	21.54	21.18	4.00	127.26	1266.96
	S28	19.19	1.27	1.95	15.57	16.38	21.43	3.66	123.04	1204.63
	D29	36.54	1.28	0.79	17.69	18.10	52.61	5.54	153.66	1354.85
	D30	37.92	1.98	0.60	17.85	21.93	51.97	5.51	140.75	1375.08
	Mean	33.30	1.93	0.92	17.30	18.98	35.38	4.62	137.25	1318.96
Overall sites (n = 30 samples)	Maximum	132.19	4.81	1.95	18.87	36.69	52.61	80.60	274.19	1393.30
	Minimum	19.19	1.27	0.29	12.22	16.38	9.48	3.66	123.04	1045.66
	Mean	66.10	2.76	0.93	14.78	26.00	32.42	26.07	201.36	1181.12
	Median	65.58	2.88	0.94	14.56	26.02	31.85	5.49	205.37	1175.88
	SD	28.75	0.87	0.38	1.70	5.49	12.03	28.39	38.77	82.78
	CV	43.49	31.54	40.50	11.52	21.10	37.11	108.89	19.26	7.01
[a] Turekian and Wedepohl (1961)		20	13	0.4	19	90	68	45	95	47,200
[b] Wedepohl (1995)		17	2	0.056	11.6	35	18.6	14.3	52	30,980
[c] Kabata-Pendias and Pendias (2001)		25	4.7	0.1	6.9	42	18	14	62	47,000

ND not detected, *CV* coefficient of variation, *SD* standard deviation, *n* number of samples

[a]Distribution of the elements in Earth's Crust in sedimentary rocks (shales)

[b]Chemical composition of the Continental Crust (Upper Continental Crust)

[c]Average HMs concentrations for world soils

or unintended by children), inhalation (e.g., oral and nasal respiratory exposure to atmospheric dust or aerosols), and dermal adsorption (Tan et al. 2018). Thus, the average daily dose (ADD, [mg/(kg/day)]) for each of the three exposure pathways was calculated using the following equations proposed by the USEPA (1989, 1996, 2011), and definitions of the abbreviations, units, and values of each parameter in these formulas are presented in Table S8.

$$ADD_{ingestion} = \frac{C_n \times IR_{ing} \times ED \times EF}{BW \times AT} \times CF \tag{7}$$

$$ADD_{inhalation} = \frac{C_n \times IR_{inh} \times ED \times EF}{BW \times AT \times PEF} \tag{8}$$

$$ADD_{dermal} = \frac{C_n \times SA \times AF \times DAF \times ED \times EF}{BW \times AT} \times CF \tag{9}$$

The United States Environmental Protection Agency (USEPA) proposed the hazard quotient (HQ) to describe the non-carcinogenic risk for each metal element single exposure pathway (USEPA 2011), which was calculated as the ratio between the average daily dose (ADD) [mg/(kg/day)] resulting from an individual exposure pathway and the corresponding reference dose (RfD) [mg/(kg/day)], as shown in Eq. 10 (Ihedioha et al. 2016). To clarify, RfD values were obtained from the Integrated Risk Information System (IRIS) database of the USEPA as an estimation for the daily exposure to the human population that does not cause deleterious effects in the human body during a lifetime (USEPA 2012) (Table S9).

$$HQ = \frac{ADD}{RfD} \tag{10}$$

The hazard index (HI) was used to estimate the non-carcinogenic cumulative risk through all exposure pathways ($HI = HQ_{ing} + HQ_{inh} + HQ_{dermal}$) (USEPA 1989). Two main categories were recognized based on HQ and HI values: (1) absence of adverse non-carcinogenic risks for HQ or HI values lower than 1, and (2) probability of potential non-carcinogenic risks for HQ or HI values higher than 1 (Diami et al. 2016; USEPA 2002b).

The carcinogenic risk assessment of HMs was employed to evaluate the degree of probability that metals could pose cancer risks to humans (Deng et al. 2019). The individual carcinogenic risk (CR) could be calculated by multiplying the average daily dose (ADD) with the cancer slope factor (CSF) as shown in the following formula (USEPA 2002b):

$$CR = ADD \times CSF \tag{11}$$

Significantly, CSF, as a carcinogen potency factor, highlights the relationship between the exposure dose and the potential response (USEPA 2011) (Table S9). Due to the unknown values of CSF for some HMs, or according to the fact that some metals are not considered to create cancer (e.g., mercury), this study evaluated the carcinogenic risks for only four metals (Pb, As, Cr, and Ni). Subsequently, the total carcinogenic risk (TCR) was estimated as the sum of the individual carcinogenic risks (CR) from the three exposure pathways for every single metal (Rahman et al. 2021) (Eq. 12). CR and TCR values below 1×10^{-6} were regarded as negligible (low carcinogenic risks), whereas values lying between 1×10^{-6} and 1×10^{-4} were considered acceptable and tolerable (moderate carcinogenic risks). Hence, the value of 1×10^{-4} was the acceptable threshold value for CR and TCR, and the exceeding values indicate the potential for lifetime carcinogenic risks (unacceptable high carcinogenic risk) (USEPA 2005).

$$TCR = \sum CR_i = CR_{inh} + CR_{ing} + CR_{dermal} \tag{12}$$

Results and discussion

Heavy metal concentrations in RD samples

The total concentration results of nine HMs in RD and basic statistical characterizations, as well as their average abundances in the earth's crust and world soil, are presented in Table 1. The mean values of Pb, As, Hg, Co, Cr, Ni, Cu, Zn, and Fe were 66.10, 2.76, 0.93, 14.78, 26.00, 32.42, 26.07, 201.36, and 1181.12 mg/kg, respectively, displaying a declining trend of Fe > Zn > Pb > Ni > Cu > Cr > Co > As > Hg. These mean values for all metals except Cu were matched with their corresponding median values, revealing that HMs followed a normal distribution. Furthermore, the coefficients of variation (CV) for all HMs (except Fe and Co) were high, demonstrating relatively high dispersion and indicating that anthropogenic activities exert an obvious and striking influence on HM levels in the RD of Greater Cairo.

During sampling, the weather was sunny and windless, with no prevailing wind direction, which explains the lack of significant spatial variation of metals between the sampling points of each street. Based on the fact that dust particles are characterized by high settlement and have a relatively short travel distance, they are mainly affected by adjacent pollution sources (Zhu et al. 2021). For instance, the relatively high Ni levels in RD samples from Sheikh Zayed City can be attributed to oil spillage due to the proximity of these locations to car maintenance shops (Taiwo et al. 2020). Moreover, sampling points with high Hg concentrations were likely to be associated with the medical wastes of nearby public and private hospitals (in old and populated urban districts) or the discharge of sewage, phosphorus fertilizers, and combustion of rubbish (in Sheikh Zayed City). Similarly, hot

spots for Pb (D16) and Zn (D17) were observed at Ramses Street in the city center owing to that this area is a transport hub, including the largest railway, metro, and unplanned bus station associated with stop-and-go traffic, on the contrary, a significant decrease was observed in the levels of traffic-related HMs (Pb, Zn, Cu, and Cr) in RD samples collected from Sheikh Zayed City (D26-D30), which was less influenced by traffic congestion and overpopulation, emphasizing the role of urban planning in reducing these traffic marker elements. Ultimately, these findings ascertain that older cities have a unique geochemical signature compared with newer cities due to the dense population, the longer erosion of the physical infrastructure (infrastructure aging), and the difference in urban design, which leads to converting the old cities into environmentally unsustainable cities (Wong et al. 2012).

In comparison with the world soil average values of Kabata-Pendias and Pendias (2001), the obtained results showed that all the studied metals had higher average contents except for Fe, As, and Cr (Table 1). Moreover, Pb and Zn mean values were higher than the average background values in shale (Turekian and Wedepohl 1961) by threefold and twofold, respectively, whereas the Zn mean value was about 17-fold the corresponding continental crust average value (Wedepohl 1995). Likewise, in a comparison between the results of this study and other cities (Table 2), the mean Hg content in this study was notably higher than those obtained from Luanda (Angola) (Ferreira-Baptista and De Miguel 2005), Nanjing (China) (Wang et al. 2020), Ahvaz (Iran) (Najmeddin et al. 2018), and Busan (South Korea) (Choi et al. 2020). Moreover, the Pb mean concentration was higher than the corresponding value in Beijing (China) (Tang et al. 2013), Dhaka (Bangladesh) (Safiur Rahman et al. 2019), and Lublin (Poland) (Zgłobicki et al. 2018). In contrast, the mean copper content of this study was the lowest among all the cities included in the comparison.

Deciphering intrarelationships and sources of HMs in RD samples

The correlation matrix, at a 0.05 significant level, revealed a strong positive correlation between Fe-Co ($r = 0.868$),

Table 2 Comparison of mean toxic metal concentrations (mg/kg) in road dust from different cities around the world

City and country	Pb	As	Hg	Co	Cr	Ni	Cu	Zn	References
Greater Cairo, Egypt	66	3	0.90	15	26	32	26	201	This study
Alexandria, Egypt	70	–	–	3	24	14	80	169	Jadoon et al. (2021)
Beijing, China	50	–	–	–	78	24	64	–	Tang et al. (2013)
Nanjing, China	102	14	0.51	11	–	–	133	281	Wang et al. (2020)
Delhi, India	121	–	–	–	149	36	192	285	Suryawanshi et al. (2016)
Dhaka, Bangladesh	19	8	–	–	144	37	50	239	Safiur Rahman et al. (2019)
Busan, South Korea	199	22	0.08	–	171	19	178	1090	Choi et al. (2020)
Ahvaz, Iran	85	–	0.32	10	52	60	74	309	Najmeddin et al. (2018)
Thessaloniki, Greece	209	–	–	–	105	89	662	453	Bourliva et al. (2017)
Luanda, Angola	351	5	0.13	3	26	10	42	317	Ferreira-Baptista and De Miguel (2005)
Lublin, Poland	44	–	–	–	86	17	82	241	Zgłobicki et al. (2018)
Madrid, Spain	1927	–	–	3	61	44	188	476	Miguel et al. (1997)
Mexico City, Mexico	128	–	–	7	51	36	100	281	Aguilera et al. (2021)

Table 3 Pearson correlation coefficients between heavy metal concentrations in road dust samples from Greater Cairo, Egypt ($n = 30$ samples)

HMs	Pb	As	Hg	Co	Cr	Ni	Cu	Zn	Fe
Pb	1								
As	0.312	1							
Hg	0.124	0.011	1						
Co	−0.129	−0.326	−0.341	1					
Cr	0.651*	0.357	−0.228	−0.021	1				
Ni	0.180	−0.372*	−0.197	0.066	0.200	1			
Cu	0.285	0.395*	0.091	−0.066	0.105	−0.589*	1		
Zn	0.733*	0.448*	−0.014	−0.246	0.775*	0.026	0.355	1	
Fe	−0.368*	−0.347	−0.274	0.868*	−0.247	0.055	−0.121	−0.431*	1

[*] Correlation is significant at the 0.05 level (two-tailed)

Zn-Cr ($r = 0.775$), and Zn-Pb ($r = 0.773$) (Table 3), whereas a moderate positive correlation was found between Cr-Pb ($r = 0.651$), inferring an interdependence and analogous origin between these metal pairs (Gurhan Yalcin 2009). The

Table 4 Rotated component matrix of HMs in RD samples from Greater Cairo, Egypt

Heavy metals	Principal components			
	PC1	PC2	PC3	PC4
Pb	**0.860**	−0.109	0.061	0.298
As	0.382	−0.328	0.581	−0.036
Hg	0.009	−0.054	−0.066	**0.982**
Co	−0.011	**0.974**	−0.057	−0.016
Cr	**0.911**	−0.022	−0.051	−0.127
Ni	0.254	0.039	−0.889	0.028
Cu	0.230	0.025	**0.850**	−0.039
Zn	**0.887**	−0.224	0.183	−0.077
Fe	−0.256	**0.923**	−0.066	−0.068
Eigenvalues	2.686	1.977	1.902	1.084
Proportion of variance %	29.845	21.971	21.136	12.041
Cumulative % of variance	29.845	51.816	72.953	84.994

Rotation Method: Varimax with Kaiser Normalization

Bold values indicate significant loading factors (> 0.7)

strong association between Fe and Co is supported by the high affinity of Co with iron hydroxides. Noteworthy, several studies have documented the predominance of natural sources (e.g., weathering of earth crust and soil-forming parent material) in Fe enrichment in RD (Al-Khashman 2007; Cai et al. 2021). On the contrary, Apeagyei et al. (2011) pointed out that traffic emissions (vehicle brake pads) could be an anthropogenic source for Fe in RD.

Principal component analysis (PCA) was performed, and the original variables were categorized into four components with eigenvalues greater than 1, which accounted for about 85% of the total variance (Table 4, Fig. 2). The first principal component (PC1) was strongly loaded with Pb, Zn, and Cr and partially loaded with As and Ni, indicating a possible source for this component being traffic-related emissions, such as tires and brake wear, as well as diesel exhaust (Idris et al. 2020). Several studies have documented that traffic-related emissions were the major contributor of Pb, Zn, and Cr in urban RD (Shi and Lu 2018). Particularly, the presence of Cr in RD was reported to be associated with plant remains, tire aging, car wheel incineration, and old car corrosion as it was used for the plating of some motor vehicle parts (chrome plating) (Ekoa Bessa et al. 2022; Jose and Srimuruganandam 2020).

Fig. 2 3D plot of the principal component analysis loadings (PCA) of HMs in Greater Cairo RD samples
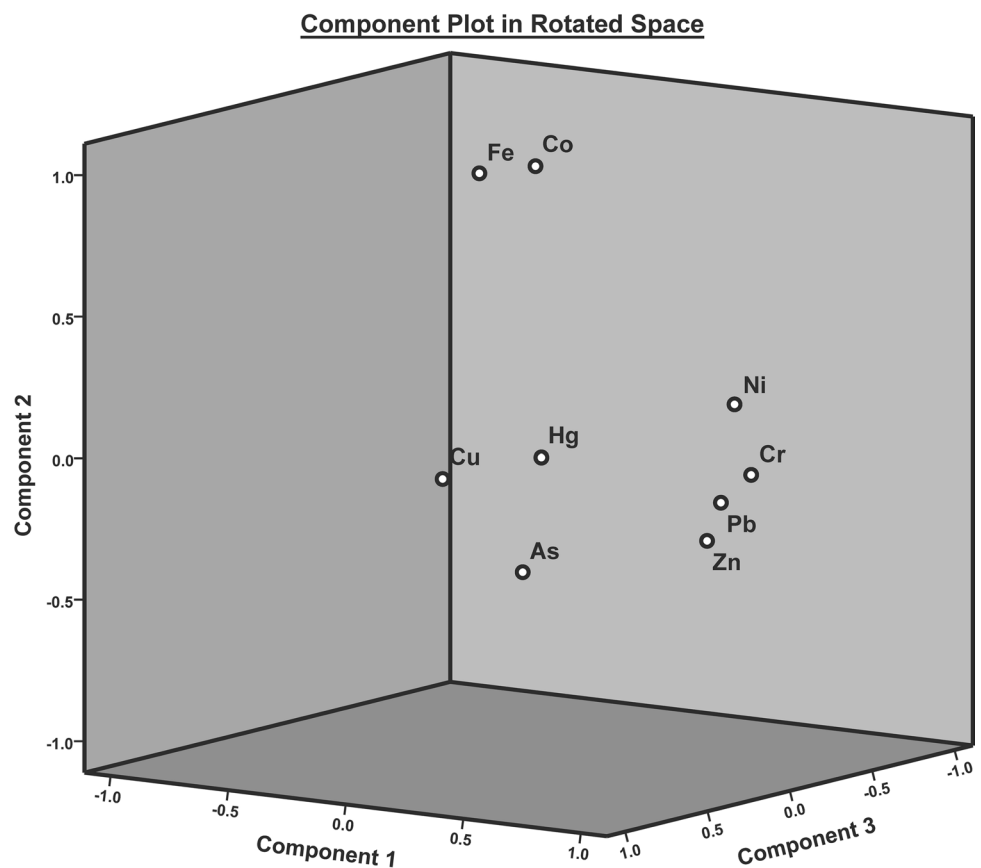
Furthermore, PC2 was dominated by Co and Fe and accounted for 21.97% of the total variance. Coupled with the high correlation between Fe and Co, PC2 can be attributed to a natural origin (crustal material and windstorm deposits). PC3 was governed by Cu and moderately by As, explaining about 21.14% of the total variance. Due to the low concentration of Cu in many sampling points, this component can be attributed to a mixed origin (natural and anthropogenic), including a combination of crustal material along with vehicle oils, mechanical abrasion of vehicles, tire abrasion, and domestic wastes (Al-Khashman, 2004; Kabir et al. 2021). The improper disposal of municipal wastes by incineration, particularly those containing batteries, colored glass, electrical cables and devices, and galvanic waste, is considered a critical source of HM (Ishchenko 2019). Notably, Cu is used in tire production to increase the adhesion between steel plies and tire rubber and in brake manufacturing to limit heat transfer (Huang et al. 2009; Kadhem et al. 2018). With regard to the PC4, it accounted for 12.04% of the total variance, including Hg with a loading value of 0.98, and its source may be linked to industrial activities and medical wastes. According to Wu and Lu (2018), it was shown that high levels of Hg in RD samples appeared in areas close to hospitals and dental clinics. Noteworthy, the moderate loading of As in different PCs revealed that its source was likely associated with more than one major factor, such as fuel burning, industrial activities, legacy input from agricultural soils

(fertilizers and pesticides), and household wastes (Masto et al. 2019; Proshad et al. 2019).

Pollution and ecological risk assessment of heavy metals in RD

The sequence of I_{geo} mean values for RD samples was Hg > Zn > Pb > Ni > As > Co > Cu > Cr (Fig. 3), with mean values of 3.34, 1.34, 1.24, 0.10, −0.19, −0.24, −0.73, −1.05, respectively. The I_{geo} values of Pb varied from −0.41 (class 0, uncontaminated) at Sheikh Zayed City to 2.37 (class 4, moderately contaminated to strongly contaminated) at Ramses Street. Moreover, all samples collected from the old Cairo districts (D1–D25) showed I_{geo} values for Zn ranging between 1 and 2, which revealed a moderate contamination grade. On the contrary, Sheikh Zayed City samples observed I_{geo} values for Zn less than 1, which exhibited uncontaminated to moderately contaminated samples. Noteworthy, the heterogeneity of I_{geo} Cu values, which ranged between (class 0, uncontaminated) and 1.91 (class 2, moderately contaminated), pointed out local hotspots and stationary point sources, which can be associated with the corrosion of metal parts and spills of waste residue (Dat et al. 2021; Guo et al. 2021). Nevertheless, nearly all samples observed negative I_{geo} values for Co and Cr, demonstrating that RD samples were uncontaminated with these metals.

The contamination factor (CF) results showed low contamination levels (CF ≤ 1) to moderate contamination levels

Fig. 3 Box plot of the geoaccumulation index (I_{geo}) for studied HMs in RD samples from Greater Cairo, Egypt
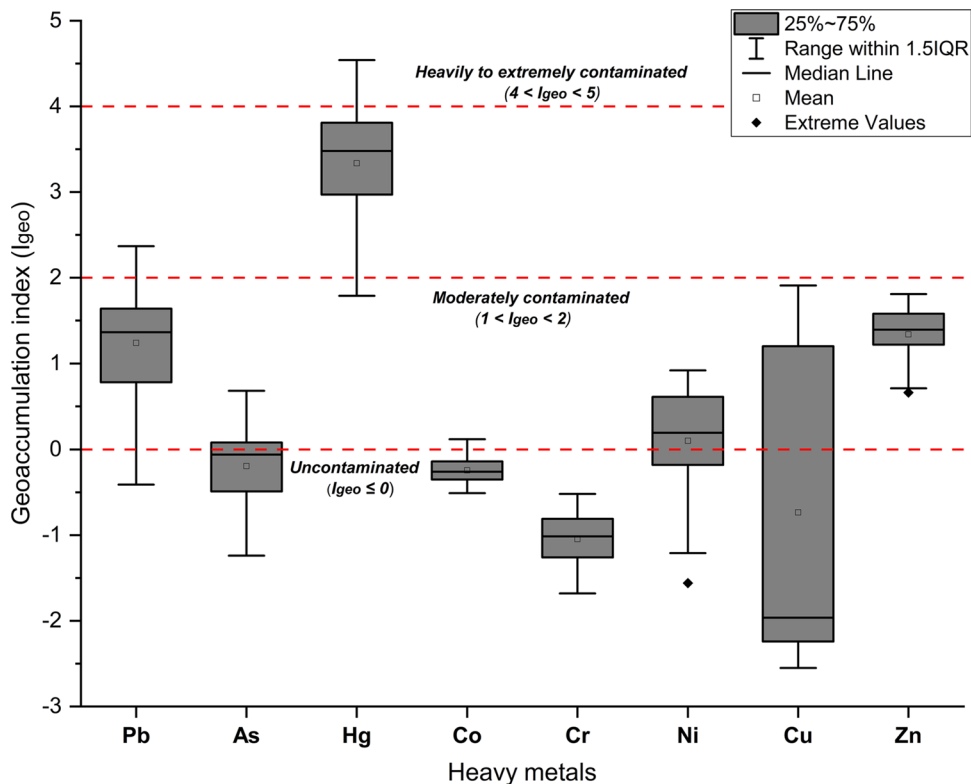
Table 5 Contamination factor (CF) and pollution load index (PLI) values for heavy metals in road dust samples from Greater Cairo, Egypt

Sites	Codes	CF								PLI
		Pb	As	Hg	Co	Cr	Ni	Cu	Zn	
Haram	D1	3.05	1.59	17.86	1.12	0.74	1.36	5.00	3.80	2.56
	D2	2.53	2.41	NC	1.22	0.65	0.70	4.42	3.48	1.76
	D3	2.58	1.10	NC	1.20	0.57	1.13	3.86	3.11	1.59
	D4	2.22	1.07	NC	1.17	0.71	1.39	0.29	3.46	1.16
	D5	2.32	1.54	10.71	1.20	0.73	1.33	0.29	3.49	1.61
	Mean	2.54	1.54	6.31	1.18	0.68	1.18	2.77	3.47	1.74
Cairo University	D6	4.06	2.01	NC	1.26	0.75	0.51	5.64	4.47	1.93
	D7	4.84	1.55	23.21	1.37	0.80	0.65	5.23	4.77	2.73
	D8	5.59	1.08	5.18	1.52	1.04	1.77	5.50	4.63	2.62
	D9	4.15	1.58	5.36	1.36	1.02	1.73	0.29	4.64	1.81
	D10	4.71	1.68	11.96	1.33	0.92	1.70	0.30	4.37	2.00
	Mean	4.67	1.58	9.34	1.37	0.90	1.27	3.39	4.58	2.22
Tahrir	D11	4.11	1.52	21.07	1.18	0.78	1.45	3.46	4.05	2.66
	D12	4.66	1.05	NC	1.37	0.80	1.82	3.28	4.87	2.06
	D13	4.10	2.03	16.79	1.22	0.85	2.32	0.32	4.51	2.17
	D14	4.06	1.20	NC	1.29	0.89	2.26	0.33	4.60	1.52
	D15	3.89	1.63	22.86	1.28	0.90	2.22	0.33	4.37	2.19
	Mean	4.17	1.48	12.54	1.27	0.85	2.01	1.54	4.48	2.12
Ramses	D16	7.78	2.00	22.50	1.17	0.69	1.54	4.86	4.22	3.12
	D17	6.62	1.97	19.64	1.18	0.87	1.88	2.90	5.27	3.05
	D18	3.99	1.11	13.75	1.33	0.80	1.87	1.82	3.61	2.31
	D19	7.75	1.59	24.11	1.25	1.05	2.55	0.34	4.26	2.49
	D20	6.84	0.74	17.50	1.27	0.80	2.41	0.37	4.07	2.06
	Mean	6.59	1.48	19.50	1.24	0.84	2.05	2.06	4.29	2.61
El-Khalifa El-Maamoun	D21	3.82	1.47	16.43	1.11	0.64	1.20	2.00	3.97	2.24
	D22	3.31	1.09	17.68	1.11	0.55	1.40	1.20	3.70	1.98
	D23	3.57	1.41	11.79	1.05	0.75	2.75	0.32	3.68	1.88
	D24	2.67	1.01	NC	1.07	0.66	2.57	0.36	3.64	1.30
	D25	3.62	1.20	19.64	1.12	0.62	2.29	0.38	3.93	1.94
	Mean	3.40	1.23	13.31	1.09	0.65	2.04	0.85	3.78	1.87
Sheikh Zayed City	D26	2.60	1.05	10.71	1.63	0.48	1.60	0.31	2.72	1.53
	D27	1.69	1.51	12.14	1.43	0.62	1.14	0.28	2.45	1.46
	S28	1.13	0.64	34.82	1.34	0.47	1.15	0.26	2.37	1.35
	D29	2.15	0.64	14.11	1.53	0.52	2.83	0.39	2.96	1.63
	D30	2.23	0.99	10.71	1.54	0.63	2.79	0.39	2.71	1.69
	Mean	1.96	0.96	16.50	1.49	0.54	1.90	0.32	2.64	1.53
Overall sites (n = 30 samples)	Mean	3.89	1.38	12.92	1.27	0.74	1.74	1.82	3.87	2.01
	Maximum	7.78	2.41	34.82	1.63	1.05	2.83	5.64	5.27	3.12
	Minimum	1.13	0.64	1.00	1.05	0.47	0.51	0.26	2.37	1.16
	SD	1.69	0.44	8.88	0.15	0.16	0.65	1.99	0.75	0.51

NC not calculated, *SD* standard deviation

$(1 > CF < 3)$ for Cr, Co, As, and Ni (Table 5). Conversely, CF values for Pb and Zn indicated a very high contamination level $(CF > 6)$ in all sampling sites except for samples collected from Sheikh Zayed City (D26-D30), in consistency with I_{geo} results, whereas all samples above the detection limit of Hg revealed a very high contamination level $(CF > 6)$. These high contamination levels can be related to high temperatures in the summer, which aggravate the release of HMs and are associated with a decrease in air turbulence in addition to accelerating tire wear and road erosion (Abbasnejad and Abbasnejad 2019; Kucbel et al. 2017). Additionally, despite banning lead in gasoline in many countries, including Egypt (since 2000), high Pb levels have still been reported in RD studies worldwide (Bourliva

et al. 2017; Christoforidis and Stamatis 2009), which can be attributed to the accumulation of Pb residues in addition to other sources, including lubricating oil, tire wear, industrial raw constituents, and construction materials (e.g., pigment and paint) (Duong and Lee 2011). Particularly, nine sampling sites observed considerable contamination with copper ($3 > CF < 6$). Presumably, tire, brake, and engine wear, heavy equipment workshops, gas stations, and motor vehicle oils are the notable and critical anthropogenic sources for Cu in RD (Kabir et al. 2021; Kadhem et al. 2018). Although copper is an essential metal nutrient for the human body, excessive copper exposure can result in many health issues, such as gastrointestinal manifestations (e.g., nausea and vomiting), liver failure, and kidney damage (Araya et al. 2007; Yang et al. 2019).

For all sampling sites, the pollution load index (PLI) values were higher than unity, which indicated the deterioration of road-dust sediment quality due to pollution by HMs (Table 5). The highest PLI values were observed at Cairo University St., Tahrir St., and Ramses St., with a maximum value recorded at the locality of D16 (Ramses St.). These sites witness seriously high traffic loads in addition to the railway line and the unplanned bus stations in their vicinity, which has become an issue for the Egyptian capital by releasing contaminants via atmospheric emissions, which then adhere to particulate matter, forming dust with a subsequent accumulation into the roadside soil and plants.

Therefore, it seemed reasonable to report that the pattern of transportation modes and traffic flow in GC impacted the enrichment of HMs in RD. Precisely, finer RD particles can be generated at high traffic loads because of the abrasion of brake pads and tiers in traffic characterized by low speeds, frequent use of brakes due to numerous stop-start maneuvers, and long periods of idling at the traffic lights (Thorpe and Harrison 2008).

Based on enrichment factor (EF) results, all calculated EF values were higher than 1.5, indicating the anthropogenic enrichment of these metals in RD sediments (Fig. 4). More precisely, EF values ranged from "significant enrichment" (Class 3) to "extremely very high enrichment" (Class 5) and the most enriched metals were Hg, Pb, Zn, and Ni ($EF > 40$), with mean values of 436.85, 103.16, 102.23, and 45.77, respectively. In this regard, Delibašić et al. (2020) reported that Ni enrichment in RD can be attributed to the combustion of diesel fuel. Furthermore, Zn, which has been known for its high mobility and bioavailability in sediments (Boussen et al. 2013), can be enriched in RD due to traffic-related emissions (e.g., use of Zn as an additive for motor oil and as a vulcanization agent to produce tires) and galvanized material erosion (e.g., road signs and vehicle metal parts) (Choi et al. 2020; Fan et al. 2021).

Concerning the ecological risks, the mean Er values for the studied HMs decreased in the following order: $Hg > Pb > As > Cu > Ni > Co > Zn > Cr$ (Table 6). Significantly,

Fig. 4 Violin plot of enrichment factor (EF) for investigated toxic HMs in RD samples from Greater Cairo, Egypt
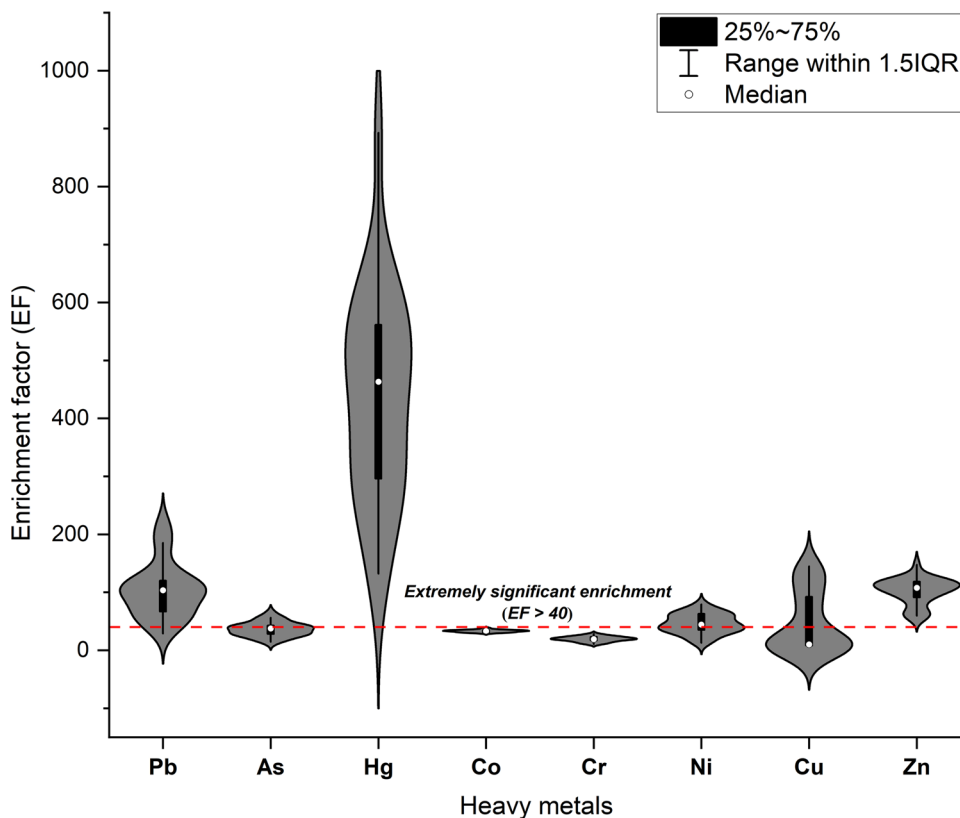
Table 6 Ecological risks results for heavy metals in road dust samples from Greater Cairo, Egypt

Sites	Codes	Er								RI
		Pb	As	Hg	Co	Cr	Ni	Cu	Zn	
Haram	D1	15.26	15.90	714.29	5.58	1.48	6.80	24.99	3.80	788.10
	D2	12.63	24.05	NC	6.10	1.30	3.51	22.08	3.48	73.16
	D3	12.90	10.95	NC	6.00	1.13	5.64	19.29	3.11	59.02
	D4	11.08	10.70	NC	5.87	1.41	6.95	1.46	3.46	40.93
	D5	11.61	15.40	428.57	6.00	1.45	6.63	1.46	3.49	474.62
	Mean	12.70	15.40	571.43	5.91	1.36	5.91	13.86	3.47	287.16
Cairo University	D6	20.30	20.05	NC	6.32	1.49	2.55	28.18	4.47	83.36
	D7	24.19	15.45	928.57	6.87	1.59	3.25	26.17	4.77	1010.86
	D8	27.97	10.75	207.14	7.58	2.08	8.87	27.49	4.63	296.50
	D9	20.76	15.80	214.29	6.81	2.04	8.65	1.47	4.64	274.44
	D10	23.56	16.80	478.57	6.63	1.84	8.48	1.48	4.37	541.73
	Mean	23.35	15.77	457.14	6.84	1.81	6.36	16.96	4.58	441.38
Tahrir	D11	20.55	15.20	842.86	5.91	1.57	7.25	17.28	4.05	914.67
	D12	23.30	10.45	NC	6.85	1.61	9.09	16.39	4.87	72.56
	D13	20.51	20.30	671.43	6.10	1.71	11.60	1.58	4.51	737.75
	D14	20.32	12.00	NC	6.45	1.78	11.29	1.65	4.60	58.09
	D15	19.47	16.25	914.29	6.38	1.79	11.09	1.64	4.37	975.28
	Mean	20.83	14.84	809.52	6.34	1.69	10.07	7.71	4.48	551.67
Ramses	D16	38.88	19.95	900.00	5.87	1.38	7.68	24.28	4.22	1002.26
	D17	33.08	19.65	785.71	5.91	1.74	9.41	14.52	5.27	875.29
	D18	19.94	11.10	550.00	6.65	1.61	9.36	9.09	3.61	611.36
	D19	38.76	15.90	964.29	6.23	2.10	12.76	1.72	4.26	1046.02
	D20	34.22	7.35	700.00	6.36	1.59	12.03	1.86	4.07	767.48
	Mean	32.97	14.79	780.00	6.21	1.68	10.25	10.30	4.29	860.48
El-Khalifa El-Maamoun	D21	19.10	14.70	657.14	5.55	1.28	6.02	10.01	3.97	717.78
	D22	16.54	10.85	707.14	5.53	1.10	6.99	6.01	3.70	757.87
	D23	17.87	14.10	471.43	5.27	1.50	13.76	1.62	3.68	529.22
	D24	13.37	10.05	NC	5.37	1.32	12.84	1.79	3.64	48.37
	D25	18.09	12.00	785.71	5.59	1.24	11.44	1.91	3.93	839.92
	Mean	16.99	12.34	655.36	5.46	1.29	10.21	4.27	3.78	578.63
Sheikh Zayed City	D26	12.99	10.45	428.57	8.13	0.97	7.98	1.54	2.72	473.36
	D27	8.44	15.05	485.71	7.13	1.23	5.69	1.40	2.45	527.09
	S28	5.64	6.35	1392.86	6.71	0.94	5.76	1.28	2.37	1421.91
	D29	10.75	6.40	564.29	7.63	1.03	14.14	1.94	2.96	609.13
	D30	11.15	9.90	428.57	7.69	1.25	13.97	1.93	2.71	477.18
	Mean	9.79	9.63	660.00	7.46	1.08	9.51	1.62	2.64	701.73
Overall sites (n = 30 samples)	Mean	19.44	13.80	661.80	6.37	1.49	8.72	9.12	3.87	570.18
	Maximum	38.88	24.05	1392.86	8.13	2.10	14.14	28.18	5.27	1421.91
	Minimum	5.64	6.35	207.14	5.27	0.94	2.55	1.28	2.37	40.93
	SD	8.46	4.35	268.03	0.73	0.31	3.23	9.93	0.75	369.41

NC not calculated, *SD* standard deviation

the calculated Er values for Hg at all sampling sites were higher than 320, inferring very high ecological risks and acting as an alarm for toxicologists. Conversely, all other metals exhibited Er values lower than 40, demonstrating low ecological risks. Considering the overall ecological risks, RI classified 50% of RD samples as having a high cumulative ecological risk (RI > 600) and about 20% as having considerable ecological risks (Table 6). Moreover, RI values ranged from 40.39 (D4, Haram St.) to 1421.91 (D28, Sheikh Zayed City), with a mean value of 570.18 (high risk), which classified Greater Cairo as a region with considerable ecological risk. Noteworthy, Hg was the main contributor to

these high ecological risks, which was evident in the significant decrease in RI values of samples in which the Hg level was below the detection limit. Accordingly, increased Hg exposure can adversely impact brain functions and the central nervous system in addition to causing cardiovascular diseases (Hagele et al. 2007; Sharifuzzaman et al. 2016). Additionally, in urban environments, HMs have other indirect implications, including the migration to water bodies through urban runoff, which affects the quality of aquatic ecosystems and increases their bioaccumulation and biomagnification in tissues of marine organisms with subsequent potential for entering the food chain (Callender and Rice 2000). Consequently, in the study area, it should also be noted that, during rainfall, metals stored in road sediments could be solubilized, dispersed, and washed off by stormwater runoff and, as a result, enter urban drainage networks and accumulate in Nile River bottom sediments, contaminating the primary source of freshwater in Egypt and posing a threat to the fluvial ecosystem. Likewise, dust storms also contribute to the relocation and dispersion of HMs in RD, with attention given to Khamasin storms, which occur seasonally in GC in the spring (Hassan and Khoder 2017).

Health risk assessment model

The average daily dose (ADD) assessment for HMs via different exposure pathways for children and adults indicated that ingestion was by far the most critical and dominantly harmful route for humans exposed to dust particles, followed by dermal contact, with inhalation being the least for both subpopulations (Table S10), which can be attributed to the greater absorption rate through the digestive system in addition to unintentionally existing in food and drink and children's hand-to-mouth practices (Li et al. 2017). In particular, the widespread presence of street food vendors in areas with very high traffic loads increases the importance of ingesting RD in GC. Furthermore, the ADD values were higher for children than adults in all exposure pathways, which is consistent with their smaller average body weight and lower averaging time under similar exposure doses. Additionally, children are more vulnerable to dust exposure as dust particles can be easily ingested through crawling and mouthing behaviors associated with outdoor play activities (Bourliva et al. 2017). These results matched those observed in previous studies (Cao et al. 2018; Ferreira-Baptista and De Miguel 2005; Shahab et al. 2020). In Greater Cairo, Robaa (2002) stated that the environmental condition in urban areas is affected by the low ventilation associated with low wind speeds compared to rural areas. Furthermore, the majority of vehicles and homes in Cairo are not air-conditioned, so car commuters and home residents have to open windows for ventilation due to the high temperatures (Jadoon et al. 2021), allowing more dust particles to enter and increasing

their inhalation exposure, especially with the majority of side streets being narrow and surrounded by tall buildings. Accordingly, people living close to urban streets, street sweepers, street vendors, traffic officers, and bus and taxi drivers, are the most vulnerable groups as they spend a significant portion of their day outdoors.

Both HQ and HI mean values for all HMs for children and adults were much less than unity, implying that the local inhabitants were not exposed to significant non-carcinogenic risks (Table 7). Despite these findings, the effect of long-term exposure should not be overlooked, so continuous monitoring is required. Regarding the carcinogenic risks, the mean CR values for adults and children through inhalation and dermal contact were below $1.0E-6$ for all metals, demonstrating low carcinogenic risks (negligible) (Fig. 5). On the contrary, Ni and Cr exhibited unacceptable high carcinogenic risks for children through ingestion ($CR > 1.0E-4$), whereas Pb and Zn showed CR values between $1.0E-6$ and $1.0E-4$, suggesting moderate carcinogenic risks (tolerable risks) (Table S11). Notably, epidemiological studies have proven increased mortality from throat, stomach, and respiratory tract cancers due to exposure to Ni and Cr (Safiur Rahman et al. 2019; Sultan et al. 2022). Likewise, TCR results for children ranged from high carcinogenic risks (Ni and Cr) to moderate carcinogenic risks (Pb and As). Unfortunately, urban areas are characterized by the proximity of the human population to pollution sources, which increases exposure rates and complicates the factors affecting public health.

Recommendations and risk management

For decades, Egypt suffered from the inefficiency of public transportation, commuting stuck in traffic, and freight transportation moving within the Greater Cairo region, considering that the size of the GC is getting bigger with the establishment of new communities associated with high migration rates from the countryside to the urban areas. Therefore, over the past years, the Egyptian government has taken several interventions to solve the transportation issues in line with Egypt Vision 2030. Among these actions were the conversion of public-sector vehicles to work with natural gas in 2004, the replacement of old taxis with modern ones, the upgrading of the Egyptian railways, the launching of new lines for the Greater Cairo metro, and the inspection of vehicle emissions as part of vehicle licensing, in addition to beginning to implement new sustainable green modes of transport (e.g., bus rapid transit (BRT) and monorail) (Hegazy et al. 2017). Despite all these steps and according to the results of this study, the environmental performance of Greater Cairo requires more effort.

Generally, dust control measures are classified into preventive strategies (to avoid the build-up of particles) and mitigating strategies (to reduce dust mobility and remove

Table 7 Non-carcinogenic risks results: Hazard quotient (HQ) and hazard index (HI) for children and adults as a result of exposure to HMs in RD samples from Greater Cairo, Egypt

HMs		HQ_{ing}		HQ_{inh}		HQ_{derm}		HI	
		Children	Adults	Children	Adults	Children	Adults	Children	Adults
Pb	Mean	2.41E−01	2.59E−02	6.73E−06	3.78E−06	4.51E−03	6.88E−04	2.46E−01	2.66E−02
	Max	4.83E−01	5.17E−02	1.35E−05	7.56E−06	9.01E−03	1.38E−03	4.92E−01	5.31E−02
	Min	7.00E−02	7.51E−03	1.95E−06	1.10E−06	1.31E−03	2.00E−04	7.13E−02	7.71E−03
As	Mean	1.18E−01	1.26E−02	8.05E−06	4.52E−06	8.03E−04	1.23E−04	1.19E−01	1.27E−02
	Max	2.05E−01	2.20E−02	1.41E−05	7.88E−06	1.40E−03	2.14E−04	2.06E−01	2.22E−02
	Min	5.40E−02	5.80E−03	3.70E−06	2.08E−06	3.70E−04	5.64E−05	5.44E−02	5.86E−03
Hg	Mean	3.96E−02	4.25E−03	3.89E−06	2.19E−06	1.59E−03	2.42E−04	4.12E−02	4.49E−03
	Max	8.30E−02	8.90E−03	8.16E−06	4.59E−06	3.32E−03	5.10E−04	8.63E−02	9.41E−03
	Min	1.24E−02	1.32E−03	1.21E−06	6.81E−07	4.95E−04	7.57E−05	1.29E−02	1.40E−03
Co	Mean	9.45E−03	1.01E−03	9.28E−04	5.21E−04	3.31E−05	5.05E−06	1.04E−02	1.54E−03
	Max	1.21E−02	1.29E−03	1.19E−03	6.65E−04	4.23E−05	6.44E−06	1.33E−02	1.96E−03
	Min	7.80E−03	8.35E−04	7.67E−04	4.31E−04	2.73E−05	4.18E−06	8.59E−03	1.27E−03
Cr	Mean	1.11E−01	1.19E−02	3.26E−04	1.83E−04	1.55E−02	2.37E−03	1.27E−01	1.45E−02
	Max	1.56E−01	1.68E−02	4.62E−04	2.58E−04	2.18E−02	3.35E−03	1.78E−01	2.04E−02
	Min	6.97E−02	7.47E−03	2.05E−04	1.15E−04	9.77E−03	1.49E−03	7.97E−02	9.08E−03
Ni	Mean	2.07E−02	2.22E−03	5.64E−07	3.17E−07	2.15E−04	3.28E−05	2.09E−02	2.25E−03
	Max	3.37E−02	3.61E−03	9.17E−07	5.15E−07	3.48E−04	5.33E−05	3.40E−02	3.66E−03
	Min	6.05E−03	6.50E−04	1.65E−07	9.27E−08	6.28E−05	9.59E−06	6.11E−03	6.60E−04
Cu	Mean	8.33E−03	8.93E−04	2.33E−07	1.31E−07	7.78E−05	1.19E−05	8.41E−03	9.05E−04
	Max	2.58E−02	2.75E−03	7.19E−07	4.03E−07	2.41E−04	3.68E−05	2.60E−02	2.79E−03
	Min	1.17E−03	1.25E−04	3.26E−08	1.83E−08	1.09E−05	1.67E−06	1.18E−03	1.27E−04
Zn	Mean	8.58E−03	9.19E−04	2.41E−07	1.35E−07	1.20E−04	1.83E−05	8.70E−03	9.37E−04
	Max	1.17E−02	1.25E−03	3.28E−07	1.84E−07	1.64E−04	2.50E−05	1.19E−02	1.28E−03
	Min	5.23E−03	5.63E−04	1.47E−07	8.27E−08	7.33E−05	1.12E−05	5.30E−03	5.74E−04

or bind dust particles). Noteworthy, the major controlling factors of RD emissions are road conditions (e.g., paving and road design), traffic characteristics and vehicle technical conditions (e.g., traffic density, vehicle speed, and vehicle type), and the surrounding environment (e.g., drainage and vegetation). Road conditions such as paving, sweeping, watering, and urban planning are among the factors affecting the generation and contamination of RD in cities. For instance, vehicle movement on unpaved roads generates more dust than on paved roads because asphalt acts as a durable surface that reduces the breakdown of soil surfaces and subsequent particle resuspension (Gulia et al. 2019). Moreover, watering the road surface is efficient in mitigating dust resuspension by reducing dust particles' mobility, increasing their mass and surface tension forces, and controlling the dust loading budget by causing particles to stick together (Denby et al. 2018), which was confirmed by Amato et al. (2012) who reported a reduction in RD mobility of 60–80% in Germany. For road washing, it can be conducted manually using hosepipes, integrated with road sweepers (e.g., water sprays with vacuum sweepers), or combined with dust chemical suppressants (e.g.,

petroleum-based binders and electrochemical stabilizers) (Amato et al. 2010; Polukarova et al. 2020). Additionally, it is also recommended that road washing should be light and regular, as less frequent and heavy watering is useless due to water evaporation. Significantly, it should be applied in the first morning hours (5–6 am) to abate the morning peak hours associated with the highest rates of emissions (7–9 am). In the same context, before developing a street cleaning plan, several considerations should be determined by the local authorities, such as the major pollutants in each region and the accumulation rate of sediment (silt loading rate), to select the most effective cleaning criteria (e.g., frequency and timing) (Gulia et al. 2019). In the study area, two types of street sweepers were noticed during fieldwork: covered and uncovered mechanical road sweepers, and the first type is recommended to be widely used to control dust particle resuspension, especially on windy days.

Traffic characteristics and vehicle technical conditions affect the rates at which RD is resuspended and released in urban environments. Hence, traffic density should be reduced by setting restrictions on vehicle weight or type, imposing ban hours for heavy vehicles, limiting motor
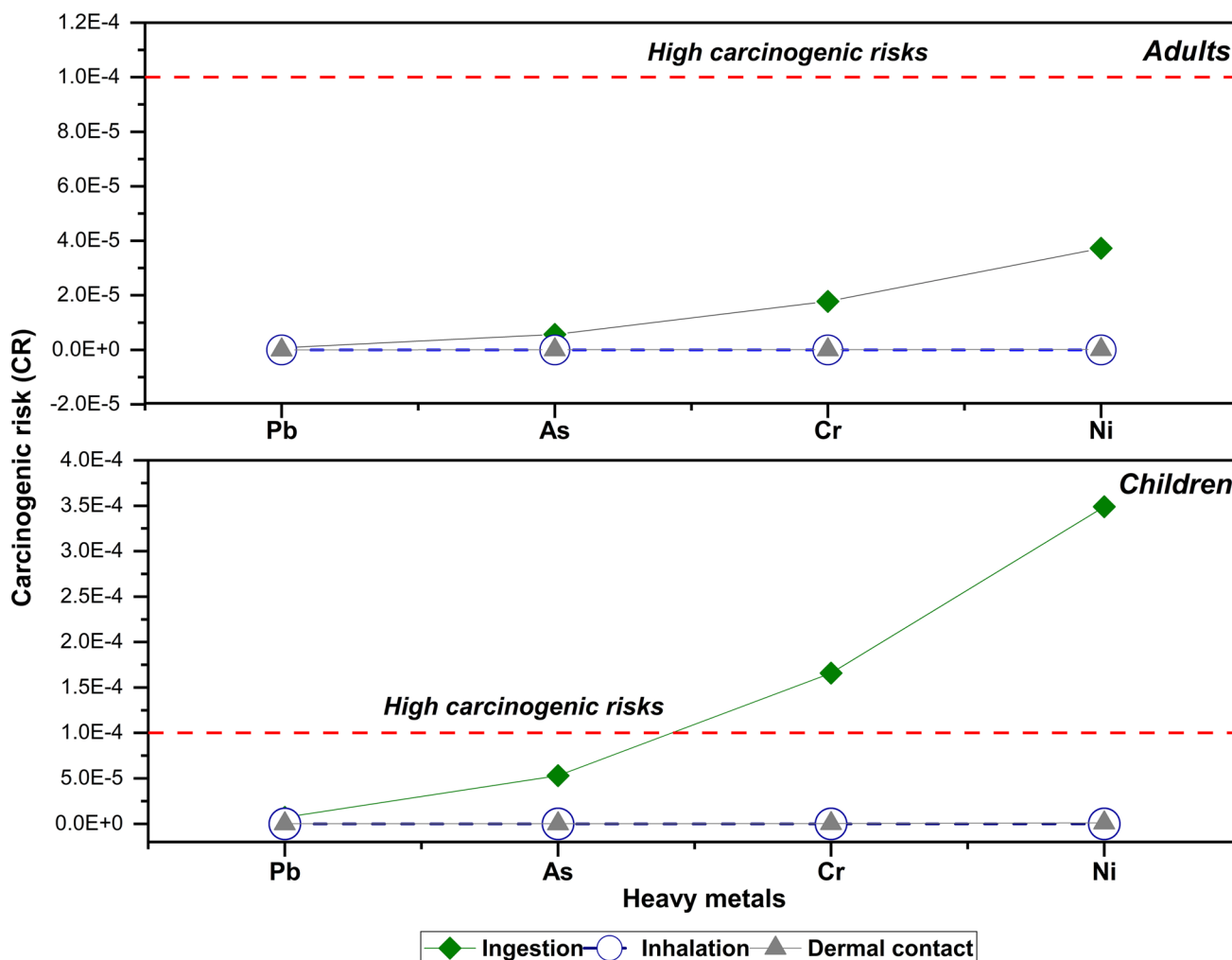
Fig. 5 Individual carcinogenic risk (CR) for children and adults posed by HMs in RD samples from Greater Cairo, Egypt

vehicle access to dirt roads, and encouraging walking. Considering the relationship between traffic emissions and vehicle type, Abu-Allaban et al. (2003) reported that heavy-duty vehicles emit 6–8 times more dust when compared to light-duty vehicles due to the high friction with the road surface, so the routes for heavy-duty vehicles should be separated in addition to limiting their movement within residential areas. Likewise, controlling tire wear helps in reducing HM release, which can be achieved by improving tire quality and enforcing speed limits using bumps and drainage channels, which is crucial as dust production and resuspension increase at high speeds, especially along unpaved roads due to on-road turbulence (Hong et al. 2020; Tong et al. 2021). Additionally, studded tires cause a higher wear effect associated with enriched metal emission levels compared to non-studded tires because of the role of stud impact and abrasion when the stud leaves the surface, which enhances vehicle grip on the road. Therefore, improving tire wear resistance and

using less-toxic elements in tire manufacturing are critical (Pirjola et al. 2009).

Enhancing the urban environment surrounding the road will also reduce dust generation rates. For instance, proper road drainage prevents the stagnation of rainwater and minimizes the accumulation of displaced soil along roadsides, whereas poor road drainage causes puddles and potholes formation due to the saturation of the roadbed by stagnating water, resulting in the need for road resurfacing. Furthermore, vegetation is an effective dust control strategy as it not only reduces the exposed ground but also holds soil particles in place by plant roots, so it is recommended to maintain the native vegetation and replant barren areas, especially with dust-absorbing green plants (Cai and Li 2019). Otherwise, we should not neglect the aspect of raising awareness about the threats of vehicle-related pollution, whether for pollution recipients or policymakers, through the launch of public awareness programs, in addition to forcing vehicle manufacturers to install particle filters and requiring drivers to use

clean filters (Abbass et al. 2020; Martins and Carrilho da Graça 2018). Ultimately, to improve the quality of life and achieve the livability of cities, several considerations should be applied in future urban planning to manage the pollution within residential blocks and learn from the experience of the past, such as integrating ecosystem planning with the social and economic aspects, stimulating industrial entities to accelerate the pace of transformation to green industries, exempting at least 30m of land on both sides of the roads from polluting human activities (Apeagyei et al. 2011), and increasing the enclosed area around construction sites inside the populated urban areas.

Conclusions

Based on the geochemical analysis, pollution indices, and multivariate statistics, HMs in RD samples collected from the Greater Cairo megacity can be classified into three categories according to their origin: natural elements, which include Fe and Co, with an evaluation as non-polluting elements; urban elements, which include Hg, Pb, and Zn, advocating a high contamination level; and mixed-source elements, which include Cu, Cr, As, and Ni, showing a moderate contamination grade. Notably, RD in the study area has multiple anthropogenic input sources, which are mainly traffic emissions, household waste incineration, and unplanned commercial and industrial activities. Ultimately, several aspects were responsible for worsening the environmental conditions in Greater Cairo, such as poor traffic conditions, a lack of urban planning, the presence of industrial workshops inside the residential areas, and the incineration of household waste. Appropriately, it may be asserted that the environmental quality is expected to continue deteriorating in light of these high population growth rates. Consequently, the results of this research will be useful in developing a road dust management program to control the input from these sources, giving priority to Hg, Pb, and Zn, with a recommendation to accelerate the use of clean energy to improve the quality of life. Additionally, further studies should address the mobilization and bioavailability of road dust, the efficiency of current street sweeping techniques, the aerodynamic behavior of road particles, and the seasonal variations in metal contents.

Author contributions MTM: conceptualization, writing—original draft; HE-N: visualization, supervision; RMG: investigation, methodology; HFA: methodology, writing—original draft; MAA: visualization, software, review and editing; SAS: investigation, formal analysis, review and editing; IHK: supervision, writing—review and editing. All authors read and approved the final manuscript.

Declarations

Conflict of interest The authors have no competing interests to declare that are relevant to the content of this article.

Ethical approval Not applicable.

Ethical approval for animal research This article does not contain any studies on animals performed by any authors.

Ethical responsibilities for authors All authors have read, understood, and have complied as applicable with the statement on "Ethical responsibilities of Authors" as found in the Instructions for Authors.

Consent to participate No human participants were involved in this study.

References

Abbasnejad A, Abbasnejad B (2019) Distribution, sources and pollution status of Pb in indoor and outdoor dusts of Kerman City, SE Iran. Environ Forensics 20(1):106–119. https://doi.org/10.1080/15275922.2019.1566289

Abbass RA, Kumar P, El-Gendy A (2020) Car users exposure to particulate matter and gaseous air pollutants in megacity Cairo. Sustain Cities Soc 56:102090. https://doi.org/10.1016/j.scs.2020.102090

Abdelhafiz MA, Elnazer AA, Seleem EMM et al (2021) Chemical and bacterial quality monitoring of the Nile River water and associated health risks in Qena-Sohag sector, Egypt. Environ Geochem Health 43:4089–4104. https://doi.org/10.1007/s10653-021-00893-3

Abou El-Anwar EA, Abdelhafiz MA, Salman SA (2022) Rare earth and trace elements enrichment and implications in black shales of Safaga-Qussier sector, Egypt. J Afr Earth Sci 188:104482. https://doi.org/10.1016/j.jafrearsci.2022.104482

Abu-Allaban M, Gillies JA, Gertler AW, Clayton R, Proffitt D (2003) Tailpipe, resuspended road dust, and brake-wear emission factors from on-road vehicles. Atmos Environ 37(37):5283–5293. https://doi.org/10.1016/j.atmosenv.2003.05.005

Adachi K, Tainosho Y (2004) Characterization of heavy metal particles embedded in tire dust. Environ Int 30(8):1009–1017. https://doi.org/10.1016/j.envint.2004.04.004

Aguilera A, Bautista F, Gutiérrez-Ruiz M, Ceniceros-Gómez AE, Cejudo R, Goguitchaichvili A (2021) Heavy metal pollution of street dust in the largest city of Mexico, sources and health risk assessment. Environ Monit Assess 193(4):193. https://doi.org/10.1007/s10661-021-08993-4

Al-Afify ADG, Othman AA, Ramadan MF (2018) Characterization of chemical and microbiological quality of Nile River surface water at Cairo (Egypt). Rendiconti Lincei Scienze Fisiche e Naturali 29(3):725–736. https://doi.org/10.1007/s12210-018-0721-8

Ali EA, Ibrahim YH, Nasralla MM (1992) Contamination of the agricultural land due to industrial activities southern of greater Cairo. J Environ Sci Health Part A 27(5):1293–1304. https://doi.org/10.1080/10934529209375797

Al-Khashman OA (2004) Heavy metal distribution in dust, street dust and soils from the work place in Karak Industrial Estate, Jordan. Atmos Environ 38(39):6803–6812. https://doi.org/10.1016/j.atmosenv.2004.09.011

Al-Khashman OA (2007) Determination of metal accumulation in deposited street dusts in Amman, Jordan. Environ Geochem Health 29(1):1–10. https://doi.org/10.1007/s10653-006-9067-8

Almeida SM, Pio CA, Freitas MC, Reis MA, Trancoso MA (2006) Source apportionment of atmospheric urban aerosol based on weekdays/weekend variability: evaluation of road re-suspended dust contribution. Atmos Environ 40(11):2058–2067. https://doi.org/10.1016/j.atmosenv.2005.11.046

Al-Shidi HK, Sulaiman H, Al-Reasi HA, Jamil F, Aslam M (2021) Human and ecological risk assessment of heavy metals in different particle sizes of road dust in Muscat, Oman. Environ Sci Pollut Res 28(26):33980–33993. https://doi.org/10.1007/s11356-020-09319-6

Amato F, Querol X, Johansson C, Nagl C, Alastuey A (2010) A review on the effectiveness of street sweeping, washing and dust suppressants as urban PM control methods. Sci Total Environ 408(16):3070–3084. https://doi.org/10.1016/j.scitotenv.2010.04.025

Amato F, Schaap M, Denier van der Gon HAC, Pandolfi M, Alastuey A, Keuken M, Querol X (2012) Effect of rain events on the mobility of road dust load in two Dutch and Spanish roads. Atmos Environ 62:352–358. https://doi.org/10.1016/j.atmosenv.2012.08.042

Apeagyei E, Bank MS, Spengler JD (2011) Distribution of heavy metals in road dust along an urban-rural gradient in Massachusetts. Atmos Environ 45(13):2310–2323. https://doi.org/10.1016/j.atmosenv.2010.11.015

Araya M, Olivares M, Pizarro F (2007) Copper in human health. Int J Environ Health 1(4):608. https://doi.org/10.1504/IJENVH.2007.018578

Bain DJ, Yesilonis ID, Pouyat RV (2012) Metal concentrations in urban riparian sediments along an urbanization gradient. Biogeochemistry 107(1–3):67–79. https://doi.org/10.1007/s10533-010-9532-4

Bernabé JM, Carretero MI, Galán E (2005) Mineralogy and origin of atmospheric particles in the industrial area of Huelva (SW Spain). Atmos Environ 39(36):6777–6789. https://doi.org/10.1016/j.atmosenv.2005.07.073

Bourliva A, Christophoridis C, Papadopoulou L, Giouri K, Papadopoulos A, Mitsika E, Fytianos K (2017) Characterization, heavy metal content and health risk assessment of urban road dusts from the historic center of the city of Thessaloniki, Greece. Environ Geochem Health 39(3):611–634. https://doi.org/10.1007/s10653-016-9836-y

Boussen S, Soubrand M, Bril H, Ouerfelli K, Abdeljaouad S (2013) Transfer of lead, zinc and cadmium from mine tailings to wheat (Triticum aestivum) in carbonated Mediterranean (Northern Tunisia) soils. Geoderma 192:227–236. https://doi.org/10.1016/j.geoderma.2012.08.029

Buat-Menard P, Chesselet R (1979) Variable influence of the atmospheric flux on the trace metal chemistry of oceanic suspended matter. Earth Planet Sci Lett 42(3):399–411. https://doi.org/10.1016/0012-821X(79)90049-9

Cai K, Li C (2019) Street dust heavy metal pollution source apportionment and sustainable management in a typical city—Shijiazhuang, China. Int J Environ Res Public Health 16(14):2625. https://doi.org/10.3390/ijerph16142625

Cai Y, Li F, Zhang J, Zhu X, Li Y, Fu J, Chen X, Liu C (2021) Toxic metals in size-fractionated road dust from typical industrial district: Seasonal distribution, bioaccessibility and stochastic-fuzzy health risk management. Environ Technol Innov 23:101643. https://doi.org/10.1016/j.eti.2021.101643

Callender E, Rice KC (2000) The urban environmental gradient: anthropogenic influences on the spatial and temporal distributions of lead and zinc in sediments. Environ Sci Technol 34(2):232–238. https://doi.org/10.1021/es990380s

Cao Z, Chen Q, Wang X, Zhang Y, Wang S, Wang M, Zhao L, Yan G, Zhang X, Zhang Z, Yang T, Shen M, Sun J (2018) Contamination characteristics of trace metals in dust from different levels of roads of a heavily air-polluted city in north China. Environ Geochem Health 40(6):2441–2452. https://doi.org/10.1007/s10653-018-0110-3

Chambers LG, Chin Y-P, Filippelli GM, Gardner CB, Herndon EM, Long DT, Lyons WB, Macpherson GL, McElmurry SP, McLean CE, Moore J, Moyer RP, Neumann K, Nezat CA, Soderberg K, Teutsch N, Widom E (2016) Developing the scientific framework for urban geochemistry. Appl Geochem 67:1–20. https://doi.org/10.1016/j.apgeochem.2016.01.005

Choi JY, Jeong H, Choi K-Y, Hong GH, Yang DB, Kim K, Ra K (2020) Source identification and implications of heavy metals in urban roads for the coastal pollution in a beach town, Busan, Korea. Mar Pollut Bull 161:111724. https://doi.org/10.1016/j.marpolbul.2020.111724

Christoforidis A, Stamatis N (2009) Heavy metal contamination in street dust and roadside soil along the major national road in Kavala's region. Greece Geoderma 151(3–4):257–263. https://doi.org/10.1016/j.geoderma.2009.04.016

Dat ND, Nguyen V-T, Vo T-D-H, Bui X-T, Bui M-H, Nguyen LSP, Nguyen X-C, Tran AT-K, Nguyen T-T-A, Ju Y-R, Huynh T-M-T, Nguyen D-H, Bui H-N, Lin C (2021) Contamination, source attribution, and potential health risks of heavy metals in street dust of a metropolitan area in Southern Vietnam. Environ Sci Pollut Res 28(36):50405–50419. https://doi.org/10.1007/s11356-021-14246-1

Davies TC (2015) Urban geology of African megacities. J Afr Earth Sc 110:188–226. https://doi.org/10.1016/j.jafrearsci.2015.06.012

Davis AP, Shokouhian M, Ni S (2001) Loading estimates of lead, copper, cadmium, and zinc in urban runoff from specific sources. Chemosphere. https://doi.org/10.1016/S0045-6535(00)00561-0

de Miguel E, Llamas JF, Chacón E, Berg T, Larssen S, Røyset O, Vadset M (1997) Origin and patterns of distribution of trace elements in street dust: unleaded petrol and urban lead. Atmos Environ 31(17):2733–2740. https://doi.org/10.1016/S1352-2310(97)00101-5

de Vos E, Edwards SJ, McDonald I, Wray DS, Carey PJ (2002) A baseline survey of the distribution and origin of platinum group elements in contemporary fluvial sediments of the Kentish Stour, England. Appl Geochem 17(8):1115–1121. https://doi.org/10.1016/S0883-2927(02)00010-0

Delibašić Š, Đokić-Kahvedžić N, Karić M, Keskin I, Velispahić A, Huremović J, Herceg K, Selimović A, Silajdžić S, Žero S, Gojak-Salimović S, Partić A, Pašalić A (2020) Health risk assessment of heavy metal contamination in street dust of federation of Bosnia

and Herzegovina. Hum Ecol Risk Assess Int J 27(5):1296–1308. https://doi.org/10.1080/10807039.2020.1826290

Denby BR, Kupiainen KJ & Gustafsson M (2018) Review of road dust emissions. In: Non-exhaust emissions, pp 183–203. Elsevier. https://doi.org/10.1016/B978-0-12-811770-5.00009-1

Deng Y, Jiang L, Xu L, Hao X, Zhang S, Xu M, Zhu P, Fu S, Liang Y, Yin H, Liu X, Bai L, Jiang H, Liu H (2019) Spatial distribution and risk assessment of heavy metals in contaminated paddy fields—a case study in Xiangtan City, southern China. Ecotoxicol Environ Saf 171:281–289. https://doi.org/10.1016/j.ecoenv.2018.12.060

Diami SM, Kusin FM, Madzin Z (2016) Potential ecological and human health risks of heavy metals in surface soils associated with iron ore mining in Pahang, Malaysia. Environ Sci Pollut Res 23(20):21086–21097. https://doi.org/10.1007/s11356-016-7314-9

Duong TTT, Lee B-K (2011) Determining contamination level of heavy metals in road dust from busy traffic areas with different characteristics. J Environ Manage 92(3):554–562. https://doi.org/10.1016/j.jenvman.2010.09.010

Ekoa Bessa AZ, Ambassa Bela V, Ngueutchoua G, El-Amier YA, Aonsi Kamani F, Ngueudong Zebaze L, Kamguem Fotso CA, Njimanu Njong V, Kemgang Ghomsi FE, Valipour M, Armstrong-Altrin JS (2022) Characteristics and source identification of environmental trace metals in beach sediments along the Littoral Zone of Cameroon. Earth Syst Environ 6(1):175–187. https://doi.org/10.1007/s41748-021-00279-6

Elnazer AA, Salman SA, Seleem EM, Abu El Ella EM (2015) Assessment of some heavy metals pollution and bioavailability in roadside soil of Alexandria-Marsa Matruh Highway, Egypt. Int J Ecol 2015:1–7. https://doi.org/10.1155/2015/689420

Fan X, Lu X, Yu B, Zuo L, Fan P, Yang Y, Zhuang S, Liu H, Qin Q (2021) Risk and sources of heavy metals and metalloids in dust from university campuses: a case study of Xi'an, China. Environ Res 202:111703. https://doi.org/10.1016/j.envres.2021.111703

Fan P, Lu X, Yu B, Fan X, Wang L, Lei K, Yang Y, Zuo L, Rinkleke J (2022) Spatial distribution, risk estimation and source apportionment of potentially toxic metal(loid)s in resuspended megacity street dust. Environ Int 160:107073. https://doi.org/10.1016/j.envint.2021.107073

Ferreira-Baptista L, De Miguel E (2005) Geochemistry and risk assessment of street dust in Luanda, Angola: a tropical urban environment. Atmos Environ 39(25):4501–4512. https://doi.org/10.1016/j.atmosenv.2005.03.026

Gad A, Saleh A, Farhat HI, Dawood YH, Abd El Bakey SM (2022) Spatial distribution, contamination levels, and health risk assessment of potentially toxic elements in household dust in Cairo City, Egypt. Toxics 10:466. https://doi.org/10.3390/toxics10080466

Gardner CB, Lyons WB, Long DT (2014) Defining urban geochemistry. Int Assoc GeoChem 95(49):460–460. https://doi.org/10.1002/2014EO490007

Gulia S, Goyal P, Goyal SK, Kumar R (2019) Re-suspension of road dust: Contribution, assessment and control through dust suppressants—a review. Int J Environ Sci Technol 16(3):1717–1728. https://doi.org/10.1007/s13762-018-2001-7

Guo G, Wu F, Xie F, Zhang R (2012) Spatial distribution and pollution assessment of heavy metals in urban soils from southwest China. J Environ Sci 24(3):410–418. https://doi.org/10.1016/S1001-0742(11)60762-6

Guo G, Zhang D, Yuntao, Wang (2021) Source apportionment and source-specific health risk assessment of heavy metals in size-fractionated road dust from a typical mining and smelting area, Gejiu, China. Environ Sci Pollut Res 28(8):9313–9326. https://doi.org/10.1007/s11356-020-11312-y

Gurhan Yalcin M (2009) Heavy mineral distribution as related to environmental conditions for modern beach sediments from the Susanoglu (Atakent, Mersin, Turkey). Environ Geol 58(1):119–129. https://doi.org/10.1007/s00254-008-1499-2

Gurjar BR, Butler TM, Lawrence MG, Lelieveld J (2008) Evaluation of emissions and air quality in megacities. Atmos Environ 42(7):1593–1606. https://doi.org/10.1016/j.atmosenv.2007.10.048

Hagele TJ, Mazerik JN, Gregory A, Kaufman B, Magalang U, Kuppusamy ML, Marsh CB, Kuppusamy P, Parinandi NL (2007) Mercury activates vascular endothelial cell phospholipase D through thiols and oxidative stress. Int J Toxicol 26(1):57–69. https://doi.org/10.1080/10915810601120509

Hakanson L (1980) An ecological risk index for aquatic pollution control a sedimentological approach. Water Res 14(8):975–1001. https://doi.org/10.1016/0043-1354(80)90143-8

Hassan SK, Khoder MI (2017) Chemical characteristics of atmospheric PM 2.5 loads during air pollution episodes in Giza, Egypt. Atmos Environ 150:346–355. https://doi.org/10.1016/j.atmosenv.2016.11.026

Hegazy I, Seddik W, Ibrahim H (2017) Towards green cities in developing countries: egyptian new cities as a case study. Int J Low-Carbon Technol 12(4):358–368. https://doi.org/10.1093/ijlct/ctx009

Hong N, Guan Y, Yang B, Zhong J, Zhu P, Ok YS, Hou D, Tsang DCW, Guan Y, Liu A (2020) Quantitative source tracking of heavy metals contained in urban road deposited sediments. J Hazard Mater 393:122362. https://doi.org/10.1016/j.jhazmat.2020.122362

Huang S, Tu J, Liu H, Hua M, Liao Q, Feng J, Weng Z, Huang G (2009) Multivariate analysis of trace element concentrations in atmospheric deposition in the Yangtze River Delta, East China. Atmos Environ 43(36):5781–5790. https://doi.org/10.1016/j.atmosenv.2009.07.055

Huzayyin AS, Salem H (2013) Analysis of thirty years evolution of urban growth, transport demand and supply, energy consumption, greenhouse and pollutants emissions in Greater Cairo. Res Transp Econ 40(1):104–115. https://doi.org/10.1016/j.retrec.2012.06.035

Idris AM, Alqahtani FMS, Said TO, Fawy KF (2020) Contamination level and risk assessment of heavy metal deposited in street dusts in Khamees-Mushait city, Saudi Arabia. Hum Ecol Risk Assess Int J 26(2):495–511. https://doi.org/10.1080/10807039.2018.1520596

Ihedioha JN, Ukoha PO, Ekere NR (2016) Ecological and human health risk assessment of heavy metal contamination in soil of a municipal solid waste dump in Uyo, Nigeria. Environ Geochem Health 39(3):497–515. https://doi.org/10.1007/s10653-016-9830-4

Irshad S, Liu G, Yousaf B et al (2019) Estimating the pollution characteristics and health risks of potentially toxic metal(loid)s in urban-industrial soils in the Indus basin, Pakistan. Environ Monit Assess 191:748. https://doi.org/10.1007/s10661-019-7909-y

Irshad S, Liu G, Yousaf B et al (2021) Geochemical fractionation and spectroscopic fingerprinting for evaluation of the environmental transformation of potentially toxic metal(oid)s in surface–subsurface soils. Environ Geochem Health 43:4329–4343. https://doi.org/10.1007/s10653-021-00932-z

Ishchenko V (2019) Heavy metals in municipal waste: the content and leaching ability by waste fraction. J Environ Sci Health Part A 54(14):1448–1456. https://doi.org/10.1080/10934529.2019.1655369

Jadoon WA, Abdel-Dayem SMMA, Saqib Z, Takeda K, Sakugawa H, Hussain M, Shah GM, Rehman W, Syed JH (2021) Heavy metals in urban dusts from Alexandria and Kafr El-Sheikh, Egypt: implications for human health. Environ Sci Pollut Res 28(2):2007–2018. https://doi.org/10.1007/s11356-020-08786-1

Jose J, Srimuruganandam B (2020) Investigation of road dust characteristics and its associated health risks from an urban environment. Environ Geochem Health 42(9):2819–2840. https://doi.org/10.1007/s10653-020-00521-6

Kabata-Pendias A, Pendias H (2001) Trace elements in soils and plants, 3rd edn. CRC Press

Kabir MdH, Kormoker T, Islam MdS, Khan R, Shammi RS, Tusher TR, Proshad R, Islam MS, Idris AM (2021) Potentially toxic elements in street dust from an urban city of a developing country: Ecological and probabilistic health risks assessment. Environ Sci Pollut Res 28(40):57126–57148. https://doi.org/10.1007/s11356-021-14581-3

Kadhem A, Yasir A, Enad M (2018) The effect of steel wire pre-tension on the tensile properties of bead ply in rubber tires. IOP Conf Ser 433:012077. https://doi.org/10.1088/1757-899X/433/1/012077

Kanakidou M, Mihalopoulos N, Kindap T, Im U, Vrekoussis M, Gerasopoulos E, Dermitzaki E, Unal A, Koçak M, Markakis K, Melas D, Kouvarakis G, Youssef AF, Richter A, Hatzianastassiou N, Hilboll A, Ebojie F, Wittrock F, von Savigny C et al (2011) Megacities as hot spots of air pollution in the East Mediterranean. Atmos Environ 45(6):1223–1235. https://doi.org/10.1016/j.atmosenv.2010.11.048

Kasimov NS, Vlasov DV, Kosheleva NE (2020) Enrichment of road dust particles and adjacent environments with metals and metalloids in eastern Moscow. Urban Climate 32:100638. https://doi.org/10.1016/j.uclim.2020.100638

Kouchou A, El Ghachtouli N, Duplay J, Ghazi M, Elsass F, Thoisy JC, Bellarbi M, Ijjaali M, Rais N (2020) Evaluation of the environmental and human health risk related to metallic contamination in agricultural soils in the Mediterranean semi-arid area (Saiss plain, Morocco). Environ Earth Sci 79(6):131. https://doi.org/10.1007/s12665-020-8880-1

Kowalska J, Mazurek R, Gąsiorek M, Setlak M, Zaleski T, Waroszewski J (2016) Soil pollution indices conditioned by medieval metallurgical activity—a case study from Krakow (Poland). Environ Pollut 218:1023–1036. https://doi.org/10.1016/j.envpol.2016.08.053

Kucbel M, Corsaro A, Švédová B, Raclavská H, Raclavský K, Juchelková D (2017) Temporal and seasonal variations of black carbon in a highly polluted European city: apportionment of potential sources and the effect of meteorological conditions. J Environ Manage 203:1178–1189. https://doi.org/10.1016/j.jenvman.2017.05.038

Li H, Shi A, Zhang X (2015) Particle size distribution and characteristics of heavy metals in road-deposited sediments from Beijing Olympic Park. J Environ Sci 32:228–237. https://doi.org/10.1016/j.jes.2014.11.014

Li H-H, Chen L-J, Yu L, Guo Z-B, Shan C-Q, Lin J-Q, Gu Y-G, Yang Z-B, Yang Y-X, Shao J-R, Zhu X-M, Cheng Z (2017) Pollution characteristics and risk assessment of human exposure to oral bioaccessibility of heavy metals via urban street dusts from different functional areas in Chengdu, China. Sci Total Environ 586:1076–1084. https://doi.org/10.1016/j.scitotenv.2017.02.092

Logiewa A, Miazgowicz A, Krennhuber K, Lanzerstorfer C (2020) Variation in the concentration of metals in road dust size fractions between 2 µm and 2 mm: results from three Metallurgical Centres in Poland. Arch Environ Contam Toxicol 78(1):46–59. https://doi.org/10.1007/s00244-019-00686-x

Lu X, Wu X, Wang Y, Chen H, Gao P, Fu Y (2014) Risk assessment of toxic metals in street dust from a medium-sized industrial city of China. Ecotoxicol Environ Saf 106:154–163. https://doi.org/10.1016/j.ecoenv.2014.04.022

Luo W, Lu Y, Giesy JP, Wang T, Shi Y, Wang G, Xing Y (2007) Effects of land use on concentrations of metals in surface soils and ecological risk around Guanting Reservoir, China.

Environ Geochem Health 29(6):459–471. https://doi.org/10.1007/s10653-007-9115-z

Maanan M, Saddik M, Maanan M, Chaibi M, Assobhei O, Zourarah B (2015) Environmental and ecological risk assessment of heavy metals in sediments of Nador lagoon, Morocco. Ecol Ind 48:616–626. https://doi.org/10.1016/j.ecolind.2014.09.034

Malakootian M, Mohammadi A, Nasiri A, Asadi AMS, Conti GO, Faraji M (2021) Spatial distribution and correlations among elements in smaller than 75 µm street dust: ecological and probabilistic health risk assessment. Environ Geochem Health 43(1):567–583. https://doi.org/10.1007/s10653-020-00694-0

Martins NR, Carrilho da Graça G (2018) Impact of PM2.5 in indoor urban environments: a review. Sustain Cities Soc 42:259–275. https://doi.org/10.1016/j.scs.2018.07.011

Masoud AA (2023) Spatio-temporal patterns and trends of the air pollution integrating MERRA-2 and in situ air quality data over Egypt (2013–2021). Air Qual Atmos Health 16:1543–1570. https://doi.org/10.1007/s11869-023-01357-6

Masto RE, Singh MK, Rout TK, Kumar A, Kumar S, George J, Selvi VA, Dutta P, Tripathi RC, Srivastava NK (2019) Health risks from PAHs and potentially toxic elements in street dust of a coal mining area in India. Environ Geochem Health 41(5):1923–1937. https://doi.org/10.1007/s10653-019-00250-5

Men C, Liu R, Wang Q, Miao Y, Wang Y, Jiao L, Li L, Cao L, Shen Z, Li Y, Crawford-Brown D (2021) Spatial-temporal characteristics, source-specific variation and uncertainty analysis of health risks associated with heavy metals in road dust in Beijing, China. Environ Pollut 278:116866. https://doi.org/10.1016/j.envpol.2021.116866

Mohammed AMF, Saleh IA, Abdel-Latif NM (2020) Evaluation of Health Risks in Cairo due to Deposited Dust Contaminated with Heavy Metals. J Hazardous Toxic Radioact Waste 24(3):04020007. https://doi.org/10.1061/(ASCE)HZ.2153-5515.0000497

Muller G (1969) Index of geoaccumulation in sediments of the Rhine River. GeoJournal 2:108–118

Najmeddin A, Keshavarzi B, Moore F, Lahijanzadeh A (2018) Source apportionment and health risk assessment of potentially toxic elements in road dust from urban industrial areas of Ahvaz megacity, Iran. Environ Geochem Health 40(4):1187–1208. https://doi.org/10.1007/s10653-017-0035-2

Pirjola L, Kupiainen KJ, Perhoniemi P, Tervahattu H, Vesala H (2009) Non-exhaust emission measurement system of the mobile laboratory SNIFFER. Atmos Environ 43(31):4703–4713. https://doi.org/10.1016/j.atmosenv.2008.08.024

Polukarova M, Markiewicz A, Björklund K, Strömvall A-M, Galfi H, Andersson Sköld Y, Gustafsson M, Järlskog I, Aronsson M (2020) Organic pollutants, nano- and microparticles in street sweeping road dust and washwater. Environ Int 135:105337. https://doi.org/10.1016/j.envint.2019.105337

Proshad R, Kormoker T, Islam S (2019) Distribution, source identification, ecological and health risks of heavy metals in surface sediments of the Rupsa River, Bangladesh. Toxin Rev 40(1):77–101. https://doi.org/10.1080/15569543.2018.1564143

Rahman MS, Kumar P, Ullah M, Jolly YN, Akhter S, Kabir J, Begum BA, Salam A (2021) Elemental analysis in surface soil and dust of roadside academic institutions in Dhaka city, Bangladesh and their impact on human health. Environ Chem Ecotoxicol 3:197–208. https://doi.org/10.1016/j.enceco.2021.06.001

Robaa SM (2002) Urban-suburban/rural differences over Greater Cairo, Egypt. Atmósfera, 157–171

Rovella N, Aly N, Comite V, Randazzo L, Fermo P, Barca D, Alvarez de Buergo M, La Russa MF (2021) The environmental impact of air pollution on the built heritage of historic Cairo (Egypt). Sci Total Environ 764:142905. https://doi.org/10.1016/j.scitotenv.2020.142905

Safiur Rahman M, Khan MDH, Jolly YN, Kabir J, Akter S, Salam A (2019) Assessing risk to human health for heavy metal contamination through street dust in the Southeast Asian Megacity: Dhaka, Bangladesh. Sci Total Environ 660:1610–1622. https://doi.org/10.1016/j.scitotenv.2018.12.425

Said I, Salman SAE-R, Samy Y, Awad SA, Melegy A, Hursthouse AS (2019) Environmental factors controlling potentially toxic element behaviour in urban soils, El Tebbin, Egypt. Environ Monitor Assess 191(5):267. https://doi.org/10.1007/s10661-019-7388-1

Shahab A, Zhang H, Ullah H, Rashid A, Rad S, Li J, Xiao H (2020) Pollution characteristics and toxicity of potentially toxic elements in road dust of a tourist city, Guilin, China: ecological and health risk assessment☆. Environ Pollut 266:115419. https://doi.org/10.1016/j.envpol.2020.115419

Sharifuzzaman SM, Rahman H, Ashekuzzaman SM, Islam MM, Chowdhury SR, Hossain MS (2016) Heavy metals accumulation in coastal sediments. In: Hasegawa H, Rahman IMdM, Rahman MA (eds) Environmental remediation technologies for metal-contaminated soils. Springer, pp 21–42. https://doi.org/10.1007/978-4-431-55759-3_2

Shi D, Lu X (2018) Accumulation degree and source apportionment of trace metals in smaller than 63 μm road dust from the areas with different land uses: a case study of Xi'an, China. Sci Total Environ 636:1211–1218. https://doi.org/10.1016/j.scitotenv.2018.04.385

Shilton VF, Booth CA, Smith JP, Giess P, Mitchell DJ, Williams CD (2005) Magnetic properties of urban street dust and their relationship with organic matter content in the West Midlands, UK. Atmos Environ 39(20):3651–3659. https://doi.org/10.1016/j.atmosenv.2005.03.005

Slezakova K, Pereira MC, Reis MA, Alvim-Ferraz MC (2007) Influence of traffic emissions on the composition of atmospheric particles of different sizes—Part 1: concentrations and elemental characterization. J Atmos Chem 58(1):55–68. https://doi.org/10.1007/s10874-007-9078-6

Sultan MB, Choudhury TR, Alam M-E, Doza MdB, Rahmana MdM (2022) Soil, dust, and leaf-based novel multi-sample approach for urban heavy metal contamination appraisals in a megacity, Dhaka, Bangladesh. Environ Adv 7:100154. https://doi.org/10.1016/j.envadv.2021.100154

Suryawanshi PV, Rajaram BS, Bhanarkar AD, Chalapati Rao CV (2016) Determining heavy metal contamination of road dust in Delh,i India. Atmósfera. https://doi.org/10.20937/ATM.2016.29.03.04

Sutherland RA (2000) Bed sediment-associated trace metals in an urban stream, Oahu Hawaii. Environ Geol 39(6):611–627. https://doi.org/10.1007/s002540050473

Suvetha M, Charles PE, Vinothkannan A, Rajaram R, Paray BA, Ali S (2022) Are we at risk because of road dust? An ecological and health risk assessment of heavy metals in a rapid growing city in South India. Environ Adv 7:100165. https://doi.org/10.1016/j.envadv.2022.100165

Taiwo AM, Musa MO, Oguntoke O, Afolabi TA, Sadiq AY, Akanji MA, Shehu MR (2020) Spatial distribution, pollution index, receptor modelling and health risk assessment of metals in road dust from Lagos metropolis, Southwestern Nigeria. Environ Adv 2:100012. https://doi.org/10.1016/j.envadv.2020.100012

Tan Z, Lu S, Zhao H, Kai X, Jiaxian P, Win MS, Yu S, Yonemochi S, Wang Q (2018) Magnetic, geochemical characterization and health risk assessment of road dust in Xuanwei and Fuyuan, China. Environ Geochem Health 40(4):1541–1555. https://doi.org/10.1007/s10653-018-0070-7

Tang R, Ma K, Zhang Y, Mao Q (2013) The spatial characteristics and pollution levels of metals in urban street dust of Beijing, China. Appl Geochem 35:88–98. https://doi.org/10.1016/j.apgeochem.2013.03.016

Thorpe A, Harrison RM (2008) Sources and properties of non-exhaust particulate matter from road traffic: a review. Sci Total Environ 400(1–3):270–282. https://doi.org/10.1016/j.scitotenv.2008.06.007

Tomlinson DL, Wilson JG, Harris CR, Jeffrey DW (1980) Problems in the assessment of heavy-metal levels in estuaries and the formation of a pollution index. Helgoländer Meeresuntersuchungen 33(1–4):566–575. https://doi.org/10.1007/BF02414780

Tong R, Fang Y, Zhang B, Wang Y, Yang X (2021) Monitoring and evaluating the control effect of dust suppressant on heavy metals based on ecological and health risks: a case study of Beijing. Environ Sci Pollut Res 28(12):14750–14763. https://doi.org/10.1007/s11356-020-11648-5

Turekian KK, Wedepohl KH (1961) Distribution of the Elements in Some Major Units of the Earth's Crust. Geol Soc Am Bull 72(2):175. https://doi.org/10.1130/0016-7606(1961)72[175:DOTEIS]2.0.CO;2

United Nations (2016) The World's Cities in 2016. UN. https://doi.org/10.18356/8519891f-en

USEPA (2011) Exposure factors handbook. U. S. Environmental Protection Agency

USEPA (1989) Risk assessment guidance for superfund. U.S. Environmental Protection Agency, Office of Emergency and Remedial Response.

USEPA (1996) Soil screening guidance: user's guide. U.S. Environmental Protection Agency: Office of Emergency and Remedial Response

USEPA (2002a) Child-specific exposure factors handbook. U.S. Environmental Protection Agency, National Center for Environmental Assessment, Office of Research and Development

USEPA (2002b) Supplemental guidance for developing soil screening levels for superfund sites. U.S. Environmental Protection Agency: Office of Emergency and Remedial Response.

USEPA (2004) Risk assessment guidance for superfund. Volume I: Human Health Evaluation Manual-part E, supplemental guidance for dermal risk assessment. U.S. Environmental Protection Agency: Office of superfund remediation and technology innovation.

USEPA (2005) Guidelines for carcinogen risk assessment. U.S. Environmental Protection Agency, Risk Assessment Forum

USEPA (2012) EPA's integrated risk information system program. U.S. Environmental Protection Agency: Office of Research and Development

Van der Kuijp TJ, Huang L, Cherry CR (2013) Health hazards of China's lead-acid battery industry: a review of its market drivers, production processes, and health impacts. Environ Health 12(1):61. https://doi.org/10.1186/1476-069X-12-61

Varol M (2011) Assessment of heavy metal contamination in sediments of the Tigris River (Turkey) using pollution indices and multivariate statistical techniques. J Hazard Mater 195:355–364. https://doi.org/10.1016/j.jhazmat.2011.08.051

Wang X, Liu E, Lin Q, Liu L, Yuan H, Li Z (2020) Occurrence, sources and health risks of toxic metal(loid)s in road dust from a mega city (Nanjing) in China. Environ Pollut 263:114518. https://doi.org/10.1016/j.envpol.2020.114518

Wedepohl KH (1995) The composition of the continental crust. Geochimicaet Cosmochimica Acta 59(7):1217–1232

Wheida A, Nasser A, El Nazer M, Borbon A, Abo El Ata GA, Abdel Wahab M, Alfaro SC (2018) Tackling the mortality from long-term exposure to outdoor air pollution in megacities: lessons from the Greater Cairo case study. Environ Res 160:223–231. https://doi.org/10.1016/j.envres.2017.09.028

Wong CI, Sharp JM, Hauwert N, Landrum J, White KM (2012) Impact of urban development on physical and chemical hydrogeology. Elements 8(6):429–434. https://doi.org/10.2113/gselements.8.6.429

Wu Y, Lu X (2018) Physicochemical properties and toxic elements in bus stop dusts from Qingyang, NW China. Sci Reports 8(1):12568. https://doi.org/10.1038/s41598-018-30452-3

Wu S, Peng S, Zhang X, Wu D, Luo W, Zhang T, Zhou S, Yang G, Wan H, Wu L (2015) Levels and health risk assessments of heavy metals in urban soils in Dongguan, China. J Geochem Explor 148:71–78. https://doi.org/10.1016/j.gexplo.2014.08.009

Yang B, Cao Y, Ren J, Wang M, Luo H, Li F (2019) Water incubation-induced fluctuating release of heavy metals in two smelter-contaminated soils. J Environ Sci 82:14–23. https://doi.org/10.1016/j.jes.2019.02.026

Zgłobicki W, Telecka M, Skupiński S, Pasierbińska A, Kozieł M (2018) Assessment of heavy metal contamination levels of street dust in the city of Lublin, E Poland. Environ Earth Sci 77(23):774. https://doi.org/10.1007/s12665-018-7969-2

Zgłobicki W, Telecka M, Skupiński S (2019) Assessment of short-term changes in street dust pollution with heavy metals in Lublin (E Poland)—levels, sources and risks. Environ Sci Pollut Res 26(34):35049–35060. https://doi.org/10.1007/s11356-019-06496-x

Zhang C, Liang Y, Lei L, Zhu G, Chen X, Jin T, Wu Q (2013) Hyper-methylations of RASAL1 and KLOTHO is associated with renal dysfunction in a Chinese population environmentally exposed to cadmium. Toxicol Appl Pharmacol 271(1):78–85. https://doi.org/10.1016/j.taap.2013.04.025

Zhang X, Zha T, Guo X, Meng G, Zhou J (2018) Spatial distribution of metal pollution of soils of Chinese provincial capital cities. Sci Total Environ 643:1502–1513. https://doi.org/10.1016/j.scitotenv.2018.06.177

Zhu X, Yu W, Li F, Liu C, Ma J, Yan J, Wang Y, Tian R (2021) Spatio-temporal distribution and source identification of heavy metals in particle size fractions of road dust from a typical industrial district. Sci Total Environ 780:146357. https://doi.org/10.1016/j.scitotenv.2021.146357

Žibret G (2019) Influences of coal mines, metallurgical plants, urbanization and lithology on the elemental composition of street dust. Environ Geochem Health 41(3):1489–1505. https://doi.org/10.1007/s10653-018-0228-3

Publisher's Note Springer Nature remains neutral with regard to jurisdictional claims in published maps and institutional affiliations.